

Constrained Dynamics for Searching Saddle Points on General Riemannian Manifolds

Yukuan Hu and Laura Grazioli

CERMICS, École des Ponts - Institut Polytechnique de Paris and Inria,
6-8 avenue Blaise Pascal, Cité Descartes, 77455 Marne-la-Vallée, France

January 16, 2026

Abstract

Finding constrained saddle points on Riemannian manifolds is significant for analyzing energy landscapes arising in physics and chemistry. Existing works have been limited to special manifolds that admit global regular level-set representations, excluding applications such as electronic excited-state calculations. In this paper, we develop a constrained saddle dynamics applicable to smooth functions on general Riemannian manifolds. Our dynamics is formulated compactly over the Grassmann bundle of the tangent bundle. By analyzing the Grassmann bundle geometry, we achieve universality via incorporating the second fundamental form, which captures variations of tangent spaces along the trajectory. We rigorously establish the local linear stability of the dynamics and the local linear convergence of the resulting algorithms. Remarkably, our analysis provides the first convergence guarantees for discretized saddle-search algorithms in manifold settings. Moreover, by respecting the intrinsic quotient structure, we remove unnecessary nondegeneracy assumptions on the eigenvalues of the Riemannian Hessian that are present in existing works. We also point out that locating saddle points can be more ill-conditioning than finding local minimizers, and requires using nonredundant parametrizations. Finally, numerical experiments on linear eigenvalue problems and electronic excited-state calculations showcase the effectiveness of the proposed algorithms and corroborate the established local theory.

1 Introduction

Finding the saddle points (SPs) of potential energy functionals is a fundamental task in various scientific and engineering applications, particularly those involving energy landscape analysis. For example, the transition states between two (meta)stable states, which are crucial in physics [31], chemistry [82], and biology [76], can be identified as index-1 SPs [2]. Higher-index SPs are useful for collective, multi-mode, or concerted transitions and play a key role in the construction of solution landscape [39, 88]. Here, an unconstrained index- k SP is a critical point where the Euclidean Hessian has exactly k negative eigenvalues. Additionally, Riemannian manifolds can naturally arise as constraint sets due to the incorporation of physical laws, such as in the Thomson problem [64, 81] and Bose-Einstein condensation [7, 12, 28]. In such cases, index- k constrained SPs can be analogously defined by using the Riemannian gradient and Hessian.

In comparison with finding local or global minimizers, locating SPs exhibits two distinct and major challenges: (1) there are always unknown descent directions at SPs, rendering off-the-shelf optimization methods unstable; (2) in general, it is impossible to construct a global merit function which is variationally minimized (or maximized) at SPs, posing significant difficulties for designing globally convergent numerical methods [50].

There have been numerous algorithmic developments concerning saddle search in the unconstrained settings, together with rigorous theoretical analyses. On the contrary, the exploration in the constrained settings has been confined to special manifolds that admit global regular level-set representations (see Eq. (4) later for definition). This limitation rules out applications such as electronic excited-state calculations [27, 69, 84], where the underlying quotient structures substantially complicate manifold representations. In some cases, omitting the quotient structures allows applying the existing methods directly. But unlike searching for local or global minimizers, this simplification can be detrimental in our context; see Example 2 and Section 5.1 later for an example involving the Stiefel and Grassmann manifolds.

In this work, we develop a constrained saddle dynamics on general Riemannian manifolds and analyze the theoretical properties of the continuous dynamics and the resulting discretized algorithms. We further demonstrate the effectiveness of algorithms through electronic excited-state calculations on standard benchmark molecular systems.

1.1 Literature review

In the following, we review the existing works for finding SPs in both unconstrained and constrained settings. Most of them primarily focus on developing *locally* convergent methods, with only few exceptions [49, 79]. Our discussions are confined to cases where objective values, first-order derivatives, and (approximate) Hessian-vector products are available, excluding direct applications of Newton-type methods [4, 6, 20, 78].

Unconstrained settings. In these cases, the numerical methods for finding the index-1 SPs can be mainly categorized into two classes: single-ended and double-ended methods. The double-ended methods (also known as the path-finding or chain-of-states methods) [41, 45, 55] are fed with two candidates of local minimizers and target at finding the minimum energy path (which passes through an index-1 SP under certain conditions by the mountain pass theorem [2]). The single-ended ones (also known as the surface walking or eigenvector-following methods) [68] start with a single initial point without *a priori* knowledge about the final state. In this work, we focus on the class of single-ended methods¹, covering the activation-relaxation technique (*nouveau*) [9, 10, 18, 22, 25, 60, 62], gentlest ascent dynamics [26, 71], (shrinking) dimer methods [42, 44, 70, 91, 92], among others [53, 65]. All the mentioned three methods can be set in the flow

$$\begin{aligned} \frac{d\mathbf{x}}{dt}(t) &= -\text{Proj}_{\mathbf{v}(t)^\perp}(\text{grad } f(\mathbf{x}(t))) + \langle \mathbf{v}(t), \text{grad } f(\mathbf{x}(t)) \rangle \mathbf{v}(t) \\ &= -R_{\mathbf{v}(t)}(\text{grad } f(\mathbf{x}(t))), \end{aligned} \quad (1)$$

where $f : \mathcal{E} \rightarrow \mathbb{R}$ is the objective (or energy) functional, $\langle \bullet, \bullet \rangle : \mathcal{E} \times \mathcal{E} \rightarrow \mathbb{R}$ is the inner product of the ambient Euclidean space, $\mathbf{v}(t) \in \mathcal{E}$ is an additional direction variable, $\text{Proj}_{\mathbf{v}(t)^\perp}$ denotes the orthogonal projection operator onto $\text{span}\{\mathbf{v}(t)\}^\perp$, defined as

$$\text{Proj}_{\mathbf{v}(t)^\perp}(\mathbf{u}) := \mathbf{u} - \langle \mathbf{v}(t), \mathbf{u} \rangle \mathbf{v}(t), \quad \forall \mathbf{u} \in \mathcal{E},$$

and $R_{\mathbf{v}(t)}$ represents the (Householder) reflection operator defined using $\mathbf{v}(t)$:

$$R_{\mathbf{v}(t)}(\mathbf{u}) := \mathbf{u} - 2 \langle \mathbf{v}(t), \mathbf{u} \rangle \mathbf{v}(t) = \text{Proj}_{\mathbf{v}(t)^\perp}(\mathbf{u}) - \langle \mathbf{v}(t), \mathbf{u} \rangle \mathbf{v}(t), \quad \forall \mathbf{u} \in \mathcal{E}.$$

Briefly speaking, instead of following the gradient flow, which leads the trajectory to a local or global minimizer, the dynamics (1) increases the objective value by climbing up along $\pm \mathbf{v}(t)$ (whose sign is determined by the angle between $\mathbf{v}(t)$ and $\text{grad } f(\mathbf{x}(t))$), while decreases the value in all the directions perpendicular to $\mathbf{v}(t)$. An effective candidate for $\mathbf{v}(t)$ is the

¹In fact, the double-ended methods are unsuitable for locating higher-index SPs by their nature and cannot be easily generalized.

normalized eigenvector corresponding to the lowest eigenvalue of the Hessian $\text{Hess } f(\mathbf{x}(t))$. In a neighborhood of a nondegenerate index-1 unconstrained SP, the dynamics (1) can then be viewed as the gradient flow of a local strongly convex merit function [30, 33], thereby providing a local stabilization for the index-1 SP. This underlies the activation-relaxation technique, where $\mathbf{v}(t)$ is the solution of

$$\min_{\mathbf{u}} \langle \mathbf{u}, \text{Hess } f(\mathbf{x}(t))[\mathbf{u}] \rangle, \quad \text{s. t. } \|\mathbf{u}\| = 1, \quad (2)$$

possibly solved approximately by Krylov subspace methods such as the Lanczos algorithm [46]. Instead of solving the \mathbf{v} -subproblem (2) directly, the gentlest ascent dynamics includes a direction dynamics to track the lowest eigenvector,

$$\frac{d\mathbf{v}}{dt}(t) = -\text{Proj}_{\mathbf{v}(t)^\perp}(\text{Hess } f(\mathbf{x}(t))[\mathbf{v}(t)]),$$

which follows from the Euler-Lagrange equation of problem (2). The (shrinking) dimer methods further approximate the Hessian-vector product through a central finite-difference scheme,

$$\text{Hess } f(\mathbf{x}(t))[\mathbf{v}(t)] \approx \frac{1}{2\ell(t)} (\text{grad } f(\mathbf{x}(t) + \ell(t)\mathbf{v}(t)) - \text{grad } f(\mathbf{x}(t) - \ell(t)\mathbf{v}(t))),$$

with $2\ell(t) > 0$ the so-called dimer length, which is sometimes driven to 0^+ as $t \rightarrow +\infty$ [91]. In recent years, there have been extensions for locating index- k unconstrained SPs [21, 26, 30, 58, 59, 71, 88, 89]. For instance, the gentlest ascent dynamics can be generalized by incorporating k direction dynamics [89], namely,

$$\begin{aligned} \frac{d\mathbf{x}}{dt}(t) &= -R_{V(t)}(\text{grad } f(\mathbf{x}(t))), \\ \frac{d\mathbf{v}_i}{dt}(t) &= -\text{Proj}_{\mathbf{v}_i(t)^\perp}(\text{Hess } f(\mathbf{x}(t))[\mathbf{v}_i(t)]) + 2 \sum_{j=1}^{i-1} \text{Proj}_{\mathbf{v}_j(t)}(\text{Hess } f(\mathbf{x}(t))[\mathbf{v}_i(t)]), \end{aligned} \quad (3)$$

$i = 1, \dots, k, \quad \text{with } V(t) := (\mathbf{v}_1(t), \dots, \mathbf{v}_k(t)),$

where $R_{V(t)}$ is the reflection operator defined using $V(t)$:

$$R_{V(t)}(\mathbf{u}) := \mathbf{u} - 2 \sum_{j=1}^k \langle \mathbf{v}_j(t), \mathbf{u} \rangle \mathbf{v}_j(t), \quad \forall \mathbf{u} \in \mathcal{E},$$

and $\text{Proj}_{\mathbf{v}_j(t)}$ refers to the orthogonal projection operator onto $\text{span}\{\mathbf{v}_j(t)\}$ ($j = 1, \dots, k$). The second term on the right-hand side of Eq. (3) is introduced to maintain the orthonormality condition $\langle \mathbf{v}_i(t), \mathbf{v}_j(t) \rangle = \delta_{ij}$ ($i, j = 1, \dots, k$), by combining the Lagrangian formalism with operator splitting. Some improvements have also been made for acceleration and stabilization, including those leveraging second-order information [18, 71, 89, 92], based on local merit functions [30, 33, 35], and incorporating additional inertial terms [58]. Some works have established the linear stability of the dynamics at unconstrained SPs [26, 50, 58, 89, 91] and the local convergence of the discretized algorithms [30, 33, 50, 58, 59, 91] under the nondegeneracy assumption. The error estimates for different discretization schemes can be found in [57, 93]. Recently, there have been some attempts dealing with stochastic and degenerate settings [23, 43, 77]. A package has been designed for solution landscape exploration and construction based on the dynamics (3) [56].

Constrained settings. The exploration in this context remains rather limited [52, 54, 87, 90, 94]. All these works consider special Riemannian manifolds induced by global defining functions, i.e.,

$$\mathcal{M} := \{\mathbf{x} \in \mathbb{R}^n \mid \mathbf{c}(\mathbf{x}) = 0\} \quad \text{with} \quad \mathbf{c}(\mathbf{x}) := (c_1(\mathbf{x}), \dots, c_q(\mathbf{x}))^\top \in \mathbb{R}^q, \quad (4)$$

where $q < n$ and the functions c_i 's are smooth and regular, in that $\text{rank}(\text{grad } \mathbf{c}(\mathbf{x})) = q$ for any $\mathbf{x} \in \mathcal{M}$ (note that $\text{grad } \mathbf{c}(\mathbf{x}) \in \mathbb{R}^{q \times n}$). In this case, a constrained saddle dynamics, targeting index- k constrained SPs, can be derived using the Lagrangian function with operator splitting as follows [87]:

$$\frac{d\mathbf{x}}{dt}(t) := -R_{\mathbf{x}(t), V(t)}(\text{grad}_{\mathcal{M}} f(\mathbf{x}(t))), \quad (5)$$

$$\begin{aligned} \frac{d\mathbf{v}_i}{dt}(t) &:= -\text{Proj}_{\mathbf{x}(t), \mathbf{v}_i(t)^\perp}(\text{Hess}_{\mathcal{M}} f(\mathbf{x}(t))[\mathbf{v}_i(t)]) + 2 \sum_{j=1}^{i-1} \text{Proj}_{\mathbf{x}(t), \mathbf{v}_j(t)}(\text{Hess}_{\mathcal{M}} f(\mathbf{x}(t))[\mathbf{v}_i(t)]) \\ &\quad - \text{grad } \mathbf{c}(\mathbf{x}(t))^\top \left(\text{grad } \mathbf{c}(\mathbf{x}(t)) \cdot \text{grad } \mathbf{c}(\mathbf{x}(t))^\top \right)^{-1} \left(\text{Hess } \mathbf{c}(\mathbf{x}(t)) \left[\frac{d\mathbf{x}}{dt}(t) \right] \right) \mathbf{v}_i(t), \quad (6) \\ i &= 1, \dots, k, \quad \text{with } V(t) := (\mathbf{v}_1(t), \dots, \mathbf{v}_k(t)), \end{aligned}$$

where the operators $\text{Proj}_{\mathbf{x}(t), \mathbf{v}_i(t)^\perp}$, $\text{Proj}_{\mathbf{x}(t), \mathbf{v}_j(t)}$, and $R_{\mathbf{x}(t), V(t)}$ are similarly defined on the tangent space $T_{\mathbf{x}(t)}\mathcal{M}$. Note that the invertibility of $\text{grad } \mathbf{c}(\mathbf{x}) \cdot \text{grad } \mathbf{c}(\mathbf{x})^\top$ follows from the full rank assumption. We also recall that

$$\text{Hess } \mathbf{c}(\mathbf{x})[\mathbf{u}] = (\text{Hess } c_1(\mathbf{x})[\mathbf{u}], \dots, \text{Hess } c_q(\mathbf{x})[\mathbf{u}])^\top \in \mathbb{R}^{q \times n}, \quad \forall \mathbf{u} \in \mathbb{R}^n.$$

Similar dynamics have been derived in [52, 54, 90]. In [87], the authors establish the linear stability of dynamics at index- k constrained SPs. That being said, we shall remark that the arguments in these works are only applicable to the special manifolds in Eq. (4), excluding the Grassmann manifolds, fixed-rank manifolds, and more general cases which find applications in, e.g., electronic excited-state calculations [27, 69, 84]. Moreover, the local convergence properties have not been investigated for the discretized algorithms due to the complication of manifold settings.

1.2 Contributions

In this article, we develop a constrained saddle dynamics (CSD) for finding index- k constrained SPs on general Riemannian manifolds. Instead of tracking the lowest k -dimensional invariant subspace of the Riemannian Hessian with k separate direction variables in $T_{\mathbf{x}(t)}\mathcal{M}$, we adopt an orthogonal projector $P(t) : T_{\mathbf{x}(t)}\mathcal{M} \rightarrow T_{\mathbf{x}(t)}\mathcal{M}$ as a single variable, respecting the inherent quotient structure. The position-projector pair $(\mathbf{x}(t), P(t))$ is treated compactly using the CSD formulated over the *Grassmann bundle* of k -planes in the tangent bundle $T\mathcal{M}$, denoted by $\text{Gr}_k(T\mathcal{M})$ (see Eq. (8) later for definition). By studying the geometry of $\text{Gr}_k(T\mathcal{M})$, we reveal that the time derivative of $P(t)$ necessarily contains a term defined by the second fundamental form of the manifold, accounting for the varying tangent spaces along the trajectory. Notably, this term vanishes in the unconstrained settings (cf. Eq. (3)) and, after horizontal lifts, reduces to the third term on the right-hand side of Eq. (6) for the special manifolds (4).

In theory, we establish the global well-definedness of the CSD (Theorem 1), its linear stability at index- k constrained SPs (Theorem 2), and the *first* local linear convergence results for the discretized algorithm in the manifold-constrained settings (Theorem 3). Moreover, compared with the existing linear stability results, our analysis removes unnecessary nondegeneracy assumptions on eigenvalues by taking into account the inherent quotient structure (Remarks 1 and 4). We also demonstrate through an example (Example 2) on the Grassmann manifold that finding constrained SPs can (1) be worse conditioned and (2) require choosing nonredundant parametrizations, in contrast to locating global or local minimizers.

Finally, we demonstrate the effectiveness of the developed algorithm on linear eigenvalue problems (Section 5.1) and electronic excited-state calculations for standard benchmark molecules (Section 5.2). We also corroborate numerically the influence of problem data and the importance of removing parametrization redundancies when searching for SPs.

Organization. This paper is organized as follows: we collect the preliminary materials in Section 2, including some fundamental concepts of Riemannian manifolds. In Section 3, we first investigate the geometry of the Grassmann bundle $\text{Gr}_k(T\mathcal{M})$, upon which the CSD is built. In Section 4, we establish the theoretical properties of the CSD as well as its discretized version. In Section 5, we report the numerical results on linear eigenvalue problems and electronic excited-state calculations. Finally, the conclusions are drawn in Section 6.

2 Preliminaries

2.1 Notations

Throughout this paper, scalars, vectors, and matrices are usually denoted by lowercase, bold lowercase, and uppercase letters, respectively. The sets or spaces are presented by calligraphic letters. In particular, we write the spaces of all $k \times k$ real symmetric and asymmetric matrices as $\mathbb{R}_{\text{sym}}^{k \times k}$ and $\mathbb{R}_{\text{asym}}^{k \times k}$, respectively. The Stiefel manifold of k -frames and the Grassmann manifold of k -planes in a vector space \mathcal{V} are denoted by $\text{St}_k(\mathcal{V})$ and $\text{Gr}_k(\mathcal{V})$, respectively. The orthogonal group of degree k is given by $\mathcal{O}(k)$. The notation “cl” means taking the closure of a set. The notations “ $\langle \bullet, \bullet \rangle$ ” and “ $\|\bullet\|$ ” calculate the inner product and norm of vectors in the ambient space. The notation “[\bullet, \bullet]” represents the commutator of two matrices, defined as $[A, B] := AB - BA$. The identity mapping over a vector space \mathcal{V} is denoted by $\text{Id}_{\mathcal{V}}$. We write the orthogonal projection operator onto a vector space \mathcal{V} as $\text{Proj}_{\mathcal{V}}$; if $\mathcal{V} = \text{span}\{\mathbf{v}\}$ or $\text{span}\{\mathbf{v}\}^\perp$ for some vector \mathbf{v} , we simply write $\text{Proj}_{\mathbf{v}}$ or $\text{Proj}_{\mathbf{v}^\perp}$. The reflection operator defined by $V = (\mathbf{v}_1, \dots, \mathbf{v}_k)$ is denoted by R_V ; if $k = 1$, we simply write $R_{\mathbf{v}}$.

For a Riemannian manifold \mathcal{M} with $\mathbf{x} \in \mathcal{M}$, the tangent space to \mathcal{M} at \mathbf{x} is denoted by $T_{\mathbf{x}}\mathcal{M}$, the normal space to \mathcal{M} at \mathbf{x} by $N_{\mathbf{x}}\mathcal{M}$, the tangent bundle of \mathcal{M} by $T\mathcal{M}$, any retraction over \mathcal{M} by Retr , the exponential mapping in particular by Exp , the Riemannian distance by $\text{dist}_{\mathcal{M}}$, and the second fundamental form at \mathbf{x} by $\Pi_{\mathbf{x}}$. These notations are sometimes equipped with additional superscripts to indicate manifolds. If \mathcal{M} is a quotient manifold and $\overline{\mathcal{M}}$ is its total space, with π the associated quotient map, the tangent space $T_{\mathbf{x}}\overline{\mathcal{M}}$ to $\overline{\mathcal{M}}$ at \mathbf{x} can be decomposed into vertical and horizontal subspaces, denoted by $\text{Ver}_{\mathbf{x}}^\pi\overline{\mathcal{M}}$ and $\text{Hor}_{\mathbf{x}}^\pi\overline{\mathcal{M}}$, respectively. A general Riemannian metric on $T_{\mathbf{x}}\mathcal{M}$ is denoted by $\langle \bullet, \bullet \rangle_{\mathbf{x}}$. The orthogonal projection and reflection operators defined over $T_{\mathbf{x}}\mathcal{M}$ are described by an additional subscript \mathbf{x} , e.g., $\text{Proj}_{\mathbf{x}, \mathbf{v}}$ and $R_{\mathbf{x}, \mathbf{v}}$. For a smooth function f , we write its differential, Euclidean gradient, and Euclidean Hessian as Df , $\text{grad } f$, and $\text{Hess } f$, respectively. If it is defined over a Riemannian manifold \mathcal{M} , its Riemannian gradient and Hessian are denoted by $\text{grad}_{\mathcal{M}} f$ and $\text{Hess}_{\mathcal{M}} f$, respectively.

The notation “ \oplus ” stands for the direct sum of two vector spaces, and “ \cong ” for the diffeomorphism between two vector spaces. When describing algorithms, we use superscripts within brackets to refer to the iteration numbers.

2.2 Fundamental concepts of Riemannian manifolds

We recall briefly some fundamental concepts of Riemannian manifolds. For interested readers, we refer to the monographs [1, 13, 47, 48]. Throughout this work, we consider a Riemannian submanifold \mathcal{M} embedded in a Euclidean space \mathcal{E} with $\dim(\mathcal{M}) = d$.

Tangent space and tangent bundle. For each $\mathbf{x} \in \mathcal{M}$, the tangent space to \mathcal{M} at \mathbf{x} is referred to as $T_{\mathbf{x}}\mathcal{M}$, which is defined as

$$T_{\mathbf{x}}\mathcal{M} := \{c'(0) \mid c : \mathbb{R} \supseteq \mathcal{I} \rightarrow \mathcal{M} \text{ smooth, } c(0) = \mathbf{x}\}.$$

The vectors in $T_{\mathbf{x}}\mathcal{M}$ are called tangent vectors to \mathcal{M} at \mathbf{x} . The tangent space $T_{\mathbf{x}}\mathcal{M}$ is endowed with the Riemannian metric induced from the inner product of the ambient Euclidean space.

For any $\mathbf{x} \in \mathcal{M}$, the orthogonal projection operator $\text{Proj}_{T_{\mathbf{x}}\mathcal{M}}$ from the ambient space onto the tangent space $T_{\mathbf{x}}\mathcal{M}$ is defined as

$$\text{Proj}_{T_{\mathbf{x}}\mathcal{M}}(\mathbf{v}) := \arg \min_{\mathbf{u}} \|\mathbf{u} - \mathbf{v}\|, \quad \forall \mathbf{v} \in \mathcal{E},$$

where $\|\bullet\| : \mathcal{E} \rightarrow \mathbb{R}_+$ refers to the norm induced by the inner product.

The tangent bundle of \mathcal{M} is denoted by $T\mathcal{M} := \{(\mathbf{x}, \mathbf{v}) \mid \mathbf{x} \in \mathcal{M}, \mathbf{v} \in T_{\mathbf{x}}\mathcal{M}\}$, i.e., the disjoint union of the tangent spaces to \mathcal{M} . On top of that, the Stiefel bundle of k -frames and the Grassmann bundle of k -planes in $T\mathcal{M}$ are respectively defined by

$$\text{St}_k(T\mathcal{M}) := \{(\mathbf{x}, V) \mid \mathbf{x} \in \mathcal{M}, V \in \text{St}_k(T_{\mathbf{x}}\mathcal{M})\}, \quad (7)$$

$$\text{Gr}_k(T\mathcal{M}) := \{(\mathbf{x}, P) \mid \mathbf{x} \in \mathcal{M}, P \in \text{Gr}_k(T_{\mathbf{x}}\mathcal{M})\}, \quad (8)$$

where $\text{St}_k(T_{\mathbf{x}}\mathcal{M})$ and $\text{Gr}_k(T_{\mathbf{x}}\mathcal{M})$ stand for the Stiefel manifold of ordered k -tuples of orthonormal vectors in $T_{\mathbf{x}}\mathcal{M}$ and the Grassmann manifold of k -dimensional linear subspaces of $T_{\mathbf{x}}\mathcal{M}$, respectively. In some contexts, $\text{St}_k(T_{\mathbf{x}}\mathcal{M})$ and $\text{Gr}_k(T_{\mathbf{x}}\mathcal{M})$ are called fibers over $\mathbf{x} \in \mathcal{M}$. When $k = 1$, $\text{Gr}_1(T\mathcal{M}) =: \mathbb{P}(T\mathcal{M})$ is called the projective bundle of $T\mathcal{M}$. From [13, Theorem 3.43], $T\mathcal{M}$ is a $2d$ -dimensional submanifold embedded in $\mathcal{E} \times \mathcal{E}$. By similar arguments, one could show that $\text{St}_k(T\mathcal{M})$ and $\text{Gr}_k(T\mathcal{M})$ are respectively $(d + kd - k(k+1)/2)$ - and $(d + k(d-k))$ -dimensional submanifolds embedded in proper ambient spaces.

Riemannian gradient and Hessian. For a smooth function f , its Riemannian gradient at $\mathbf{x} \in \mathcal{M}$, denoted by $\text{grad}_{\mathcal{M}} f(\mathbf{x})$, is defined as the unique element of $T_{\mathbf{x}}\mathcal{M}$ satisfying

$$\langle \text{grad}_{\mathcal{M}} f(\mathbf{x}), \mathbf{v} \rangle = Df(\mathbf{x})[\mathbf{v}], \quad \forall \mathbf{v} \in T_{\mathbf{x}}\mathcal{M},$$

where $Df(\mathbf{x})[\mathbf{v}]$ stands for the directional derivative of f at \mathbf{x} along the tangent vector \mathbf{v} . Since \mathcal{M} is a Riemannian submanifold embedded in a Euclidean space, $\text{grad}_{\mathcal{M}} f(\mathbf{x})$ can be readily computed via

$$\text{grad}_{\mathcal{M}} f(\mathbf{x}) = \text{Proj}_{T_{\mathbf{x}}\mathcal{M}}(\text{grad } f(\mathbf{x})).$$

The definition of Riemannian Hessian in the general cases necessitates the concept of Riemannian connection [13, Section 5.4]. Again due to the fact that \mathcal{M} is an embedded Riemannian submanifold in \mathcal{E} , we recall for simplicity the following characterization:

$$\text{Hess}_{\mathcal{M}} f(\mathbf{x})[\mathbf{v}] = \text{Proj}_{T_{\mathbf{x}}\mathcal{M}}(D\bar{G}(\mathbf{x})[\mathbf{v}]), \quad (9)$$

where \bar{G} is any smooth extension of $\text{grad}_{\mathcal{M}} f$ to a neighborhood of \mathcal{M} in \mathcal{E} .

Retraction. A retraction over \mathcal{M} is a smooth mapping $\text{Retr} : T\mathcal{M} \rightarrow \mathcal{M}$, $T\mathcal{M} \ni (\mathbf{x}, \mathbf{v}) \mapsto \text{Retr}_{\mathbf{x}}(\mathbf{v}) \in \mathcal{M}$, satisfying $\text{Retr}_{\mathbf{x}}(0) = \mathbf{x}$ and that $D\text{Retr}_{\mathbf{x}}(0)$ is the identity mapping on $T_{\mathbf{x}}\mathcal{M}$ for any $\mathbf{x} \in \mathcal{M}$. By leveraging the retraction, we can obtain a point by moving away from $\mathbf{x} \in \mathcal{M}$ along some $\mathbf{v} \in T_{\mathbf{x}}\mathcal{M}$, while remaining on \mathcal{M} . It follows that, it defines an update rule to preserve the feasibility. One typical example of retraction is the exponential mapping, denoted specially by $\text{Exp} : T\mathcal{M} \rightarrow \mathcal{M}$, which is determined by a set of second-order ordinary differential equations and yields geodesics over \mathcal{M} . If \mathcal{M} is complete, then it holds that [13, Proposition 10.22]

$$\text{dist}_{\mathcal{M}}(\mathbf{x}, \text{Exp}_{\mathbf{x}}(\mathbf{v})) = \|\mathbf{v}\|, \quad \forall (\mathbf{x}, \mathbf{v}) \in T\mathcal{M},$$

where $\text{dist}_{\mathcal{M}}(\bullet, \bullet) : \mathcal{M} \times \mathcal{M} \rightarrow \mathbb{R}_+$ represents the Riemannian distance over \mathcal{M} :

$$\text{dist}_{\mathcal{M}}(\mathbf{x}, \mathbf{y}) := \inf_c \left\{ \int_a^b \|c'(t)\| dt \mid c : [a, b] \rightarrow \mathcal{M} \text{ piecewise smooth, } c(a) = \mathbf{x}, c(b) = \mathbf{y} \right\}.$$

Second fundamental form. For a given $\mathbf{x} \in \mathcal{M}$, the normal space $N_{\mathbf{x}}\mathcal{M}$ is the orthogonal complement of $T_{\mathbf{x}}\mathcal{M}$ in \mathcal{E} . The second fundamental form at \mathbf{x} can be identified as the mapping $\Pi_{\mathbf{x}} : T_{\mathbf{x}}\mathcal{M} \times T_{\mathbf{x}}\mathcal{M} \rightarrow N_{\mathbf{x}}\mathcal{M}$ defined as $\Pi_{\mathbf{x}}(\mathbf{u}, \mathbf{v}) := P_{\mathbf{x}, \mathbf{u}}(\mathbf{v})$ for any $\mathbf{u}, \mathbf{v} \in T_{\mathbf{x}}\mathcal{M}$, where

$$P_{\mathbf{x}, \mathbf{u}} := D(\mathbf{y} \mapsto \text{Proj}_{T_{\mathbf{y}}\mathcal{M}})(\mathbf{x})[\mathbf{u}], \quad (10)$$

namely, the directional derivative of $\mathbf{y} \mapsto \text{Proj}_{T_{\mathbf{y}}\mathcal{M}}$ at \mathbf{x} along \mathbf{u} . That the range of $\Pi_{\mathbf{x}}$ is $N_{\mathbf{x}}\mathcal{M}$ can be shown by taking the directional derivative on the both sides of the identity $\text{Proj}_{T_{\mathbf{x}}\mathcal{M}} \circ \text{Proj}_{T_{\mathbf{x}}\mathcal{M}} = \text{Proj}_{T_{\mathbf{x}}\mathcal{M}}$, which yields

$$P_{\mathbf{x}, \mathbf{u}} \circ \text{Proj}_{N_{\mathbf{x}}\mathcal{M}} = \text{Proj}_{T_{\mathbf{x}}\mathcal{M}} \circ P_{\mathbf{x}, \mathbf{u}}, \quad P_{\mathbf{x}, \mathbf{u}} \circ \text{Proj}_{T_{\mathbf{x}}\mathcal{M}} = \text{Proj}_{N_{\mathbf{x}}\mathcal{M}} \circ P_{\mathbf{x}, \mathbf{u}}. \quad (11)$$

By the above definition, the second fundamental form accounts for the changes in the way the tangent spaces sit inside the ambient \mathcal{E} .

3 Algorithmic developments

In this section, we develop a constrained saddle dynamics (CSD) for locating index- k constrained SPs on general Riemannian manifolds. Existing works [52, 54, 87] are restricted to the special manifolds in Eq. (4) and introduce k different direction dynamics to track the lowest k -dimensional invariant subspace of Riemannian Hessian. The resulted dynamics can be placed on the Stiefel bundle $\text{St}_k(T\mathcal{M})$ (cf. Eq. (7)), which has not been recognized before. However, it is not difficult to observe the quotient structure under the hood: only the subspace is pursued and it is invariant under the choice of orthonormal basis. Therefore, we instead adopt a single dynamics of an orthogonal projector, which, together with the position dynamics, will amount to the CSD over the Grassmann bundle $\text{Gr}_k(T\mathcal{M})$ (see Section 3.2). To this end, we first investigate the geometries of $\text{St}_k(T\mathcal{M})$ and $\text{Gr}_k(T\mathcal{M})$ (see Section 3.1), which are applicable to general Riemannian manifolds. For notational ease, we assume that $\mathcal{E} = \mathbb{R}^n$ unless stated otherwise. Nevertheless, our arguments apply to general cases.

3.1 Geometries of $\text{St}_k(T\mathcal{M})$ and $\text{Gr}_k(T\mathcal{M})$

We start with the characterization of the tangent space to $\text{St}_k(T\mathcal{M})$.

Lemma 1 (Tangent space to $\text{St}_k(T\mathcal{M})$). *Let \mathcal{M} be a Riemannian submanifold of a Euclidean space \mathcal{E} with $\dim(\mathcal{M}) = d$. For any $(\mathbf{x}, V) \in \text{St}_k(T\mathcal{M})$, the tangent space*

$$T_{(\mathbf{x}, V)}\text{St}_k(T\mathcal{M}) = \left\{ (\boldsymbol{\delta}, \Gamma) \left| \begin{array}{l} \boldsymbol{\delta} \in T_{\mathbf{x}}\mathcal{M}, A \in \mathbb{R}_{\text{asym}}^{k \times k}, B \in \mathbb{R}^{(d-k) \times k} \\ \Gamma = VA + V_{\perp}B + (\Pi_{\mathbf{x}}(\boldsymbol{\delta}, \mathbf{v}_1), \dots, \Pi_{\mathbf{x}}(\boldsymbol{\delta}, \mathbf{v}_k)) \end{array} \right. \right\}, \quad (12)$$

where $V_{\perp} \in \text{St}_{d-k}(T_{\mathbf{x}}\mathcal{M})$ satisfies $V^{\top}V_{\perp} = 0$. The characterization (12) is independent from the choice of V_{\perp} .

Proof. For any $(\boldsymbol{\delta}, \Gamma) \in T_{(\mathbf{x}, V)}\text{St}_k(T\mathcal{M})$, take a smooth curve $c := (c_1, c_2) : \mathbb{R} \supseteq \mathcal{I} \rightarrow \text{St}_k(T\mathcal{M})$ over $\text{St}_k(T\mathcal{M})$ such that $c(0) = (\mathbf{x}, V)$ and $c'(0) = (\boldsymbol{\delta}, \Gamma)$. It is obvious that c_1 is a smooth curve over \mathcal{M} passing through \mathbf{x} at the origin, which implies $\boldsymbol{\delta} \in T_{\mathbf{x}}\mathcal{M}$. For the second part, note that $c_2(s)^{\top}c_2(s) = I_d$ and $c_2(s)_j = \text{Proj}_{T_{c_1(s)}\mathcal{M}}(c_2(s)_j)$, where $c_2(s)_j$ refers to the j -th column of $c_2(s)$ ($j = 1, \dots, k$). It therefore holds by the product rule that $\Gamma^{\top}V + V^{\top}\Gamma = 0$ and

$$\begin{aligned} \Gamma_j &= \frac{dc_2(s)_j}{ds} \Big|_{s=0} = \frac{d}{ds} \text{Proj}_{T_{c_1(s)}\mathcal{M}} \Big|_{s=0} (\mathbf{v}_j) + \text{Proj}_{T_{\mathbf{x}}\mathcal{M}}(\Gamma_j) \\ &= \text{Proj}_{T_{\mathbf{x}}\mathcal{M}}(\Gamma_j) + \Pi_{\mathbf{x}}(\boldsymbol{\delta}, \mathbf{v}_j), \end{aligned} \quad (13)$$

for $j = 1, \dots, k$. Since the columns of V and V_\perp constitute an orthonormal basis of $T_{\mathbf{x}}\mathcal{M}$, we have

$$(\text{Proj}_{T_{\mathbf{x}}\mathcal{M}}(\Gamma_1), \dots, \text{Proj}_{T_{\mathbf{x}}\mathcal{M}}(\Gamma_k)) = VA + V_\perp B$$

for some $A \in \mathbb{R}^{k \times k}$ and $B \in \mathbb{R}^{(d-k) \times k}$. Plugging this and Eq. (13) into $\Gamma^\top V + V^\top \Gamma = 0$ yields $A \in \mathbb{R}_{\text{asym}}^{k \times k}$ because $V^\top V_\perp = 0$ and $\Pi_{\mathbf{x}}(\delta, \mathbf{v}_j) \in N_{\mathbf{x}}\mathcal{M}$ (see Section 2.2). The proof is complete by noticing the arbitrariness of (δ, Γ) . \square

By the definitions in Eqs. (7) and (8), there is a natural projection $\pi : \text{St}_k(T\mathcal{M}) \rightarrow \text{Gr}_k(T\mathcal{M})$, defined as

$$\text{St}_k(T\mathcal{M}) \ni (\mathbf{x}, V) \mapsto \pi(\mathbf{x}, V) := (\mathbf{x}, VV^\top) \in \text{Gr}_k(T\mathcal{M}),$$

which is smooth and surjective, thus a submersion; in fact, we have the quotient structure

$$\text{Gr}_k(T\mathcal{M}) \cong \text{St}_k(T\mathcal{M})/\mathcal{O}(k). \quad (14)$$

Therefore, the tangent space to $\text{Gr}_k(T\mathcal{M})$ at (\mathbf{x}, P) can be readily obtained by computing the range of $D\pi(\mathbf{x}, V)$, where $V \in \text{St}_k(T_{\mathbf{x}}\mathcal{M})$ satisfies $P = VV^\top$. This is given in the following lemma without proof.

Lemma 2 (Tangent space to $\text{Gr}_k(T\mathcal{M})$). *Let \mathcal{M} be a Riemannian submanifold a Euclidean space \mathcal{E} with $\dim(\mathcal{M}) = d$. For any $(\mathbf{x}, P) \in \text{Gr}_k(T\mathcal{M})$, the tangent space*

$$\begin{aligned} T_{(\mathbf{x}, P)}\text{Gr}_k(T\mathcal{M}) &= \left\{ (\delta, \Delta) \mid \delta \in T_{\mathbf{x}}\mathcal{M}, \Delta = \text{Proj}_{T_{\mathbf{x}}\mathcal{M}} \circ \Delta \circ \text{Proj}_{T_{\mathbf{x}}\mathcal{M}} + \widehat{\Pi}_{\mathbf{x}}(\delta, P) \right\} \\ &= \left\{ (\delta, \Delta) \mid \delta \in T_{\mathbf{x}}\mathcal{M}, \Delta = V_\perp B V^\top + V B^\top V_\perp^\top + \widehat{\Pi}_{\mathbf{x}}(\delta, P), B \in \mathbb{R}^{(d-k) \times k} \right\}, \end{aligned} \quad (15)$$

where $V := (\mathbf{v}_1, \dots, \mathbf{v}_k) \in \text{St}_k(T_{\mathbf{x}}\mathcal{M})$ and $V_\perp := (\mathbf{v}_{k+1}, \dots, \mathbf{v}_d) \in \text{St}_{d-k}(T_{\mathbf{x}}\mathcal{M})$ satisfy $P = VV^\top$ and $V^\top V_\perp = 0$, the operator $\widehat{\Pi}_{\mathbf{x}}$ is defined by

$$\widehat{\Pi}_{\mathbf{x}}(\mathbf{u}, Q) := \sum_{\ell=1}^k \Pi_{\mathbf{x}}(\mathbf{u}, \mathbf{u}_\ell) \mathbf{u}_\ell^\top + \sum_{\ell=1}^k \mathbf{u}_\ell \Pi_{\mathbf{x}}(\mathbf{u}, \mathbf{u}_\ell)^\top, \quad (16)$$

for any $\mathbf{u} \in T_{\mathbf{x}}\mathcal{M}$ and $Q = UU^\top \in \text{Gr}_k(T_{\mathbf{x}}\mathcal{M})$ with $U := (\mathbf{u}_1, \dots, \mathbf{u}_k) \in \text{St}_k(T_{\mathbf{x}}\mathcal{M})$. The characterization (15) is independent from the choices of V and V_\perp .

A natural basis for $T_{(\mathbf{x}, V)}\text{Gr}_k(T\mathcal{M})$ is $\{(\delta_q, \Delta_q)\}_{q=1}^d \cup \{(\delta_{ij}, \Delta_{ij})\}_{i=1, \dots, k, j=k+1, \dots, d}$, where

$$(\delta_q, \Delta_q) := \left(\mathbf{v}_q, \widehat{\Pi}_{\mathbf{x}}(\mathbf{v}_q, P) \right), \quad q = 1, \dots, d, \quad (17)$$

and

$$(\delta_{ij}, \Delta_{ij}) := \left(0, \frac{1}{\sqrt{2}} (\mathbf{v}_i \mathbf{v}_j^\top + \mathbf{v}_j \mathbf{v}_i^\top) \right), \quad i = 1, \dots, k, j = k+1, \dots, d. \quad (18)$$

By virtue of the quotient structure (14), each tangent space to $\text{St}_k(T\mathcal{M})$ can be decomposed into vertical and horizontal parts induced by π .

Lemma 3 (Decomposition of the tangent space to $\text{St}_k(T\mathcal{M})$). *Let \mathcal{M} be a Riemannian submanifold of a Euclidean space \mathcal{E} with $\dim(\mathcal{M}) = d$. For any $(\mathbf{x}, V) \in \text{St}_k(T\mathcal{M})$, the tangent space to $\text{St}_k(T\mathcal{M})$ at (\mathbf{x}, V) admits a direct sum decomposition as*

$$T_{(\mathbf{x}, V)}\text{St}_k(T\mathcal{M}) = \text{Ver}_{(\mathbf{x}, V)}^\pi \text{St}_k(T\mathcal{M}) \oplus \text{Hor}_{(\mathbf{x}, V)}^\pi \text{St}_k(T\mathcal{M}),$$

where

$$\text{Ver}_{(\mathbf{x}, V)}^\pi \text{St}_k(T\mathcal{M}) := \left\{ (0, VA) \mid A \in \mathbb{R}_{\text{asym}}^{k \times k} \right\},$$

$$\text{Hor}_{(\mathbf{x}, V)}^\pi \text{St}_k(\text{T}\mathcal{M}) := \left\{ (\boldsymbol{\delta}, V_\perp B + (\Pi_{\mathbf{x}}(\boldsymbol{\delta}, \mathbf{v}_1), \dots, \Pi_{\mathbf{x}}(\boldsymbol{\delta}, \mathbf{v}_k))) \mid \boldsymbol{\delta} \in \text{T}_{\mathbf{x}}\mathcal{M}, B \in \mathbb{R}^{(d-k) \times k} \right\}$$

represent the vertical and horizontal subspaces of $\text{T}_{(\mathbf{x}, V)} \text{St}_k(\text{T}\mathcal{M})$ induced by π , respectively, and $V_\perp \in \text{St}_{d-k}(\text{T}_{\mathbf{x}}\mathcal{M})$ satisfies $V^\top V_\perp = 0$. The characterization of the horizontal subspace is independent from the choice of V_\perp . Moreover,

$$\text{Hor}_{(\mathbf{x}, V)}^\pi \text{St}_k(\text{T}\mathcal{M}) \cong \text{T}_{(\mathbf{x}, VV^\top)} \text{Gr}_k(\text{T}\mathcal{M}).$$

For any $(\boldsymbol{\delta}, \Delta) \in \text{T}_{(\mathbf{x}, VV^\top)} \text{Gr}_k(\text{T}\mathcal{M})$, its horizontal lift is $(\boldsymbol{\delta}, \Delta V) \in \text{Hor}_{(\mathbf{x}, V)}^\pi \text{St}_k(\text{T}\mathcal{M})$.

Proof. By definition, $\text{Ver}_{(\mathbf{x}, V)}^\pi \text{St}_k(\text{T}\mathcal{M}) = \ker(\text{D}\pi(\mathbf{x}, V))$. Since

$$\text{D}\pi(\mathbf{x}, V)[(\boldsymbol{\delta}, \Gamma)] = (\boldsymbol{\delta}, V\Gamma^\top + \Gamma V^\top), \quad \forall (\boldsymbol{\delta}, \Gamma) \in \text{T}_{(\mathbf{x}, V)} \text{St}_k(\text{T}\mathcal{M}),$$

and recall the characterization (12), we have for $(\boldsymbol{\delta}, \Gamma) \in \text{Ver}_{(\mathbf{x}, V)}^\pi \text{St}_k(\text{T}\mathcal{M})$ that $\boldsymbol{\delta} = 0$ and

$$V_\perp B V^\top + V B^\top V_\perp^\top = 0 \Leftrightarrow (V, V_\perp) \begin{pmatrix} B^\top \\ B \end{pmatrix} \begin{pmatrix} V^\top \\ V_\perp^\top \end{pmatrix} = 0.$$

Note that the terms involving the second fundamental form vanish due to $\boldsymbol{\delta} = 0$. Since the columns of V and V_\perp form an orthonormal basis of $\text{T}_{\mathbf{x}}\mathcal{M}$, the above equation implies that $B = 0$. Therefore, $\Gamma = VA$ for some $A \in \mathbb{R}_{\text{asym}}^{k \times k}$. This verifies the expression for the vertical subspace. Again by the characterization (12), the horizontal subspace is clear since it is the orthogonal complement of the vertical subspace. The proof is complete. \square

It is known that a natural Riemannian metric for the tangent bundle is the Sasaki metric [66, 74]. Basically, the Sasaki metric uses the Riemannian connection of \mathcal{M} to split the tangent space to $\text{T}\mathcal{M}$ at any point into horizontal and vertical subspaces, then defines the inner product using the original metric on each piece. Below, we define a Sasaki-type metric for $\text{Gr}_k(\text{T}\mathcal{M})$.

Definition 1 (Sasaki-type metric for $\text{Gr}_k(\text{T}\mathcal{M})$). *Let \mathcal{M} be a Riemannian submanifold of a Euclidean space \mathcal{E} with $\dim(\mathcal{M}) = d$. For any $(\mathbf{x}, P) \in \text{Gr}_k(\text{T}\mathcal{M})$, the Sasaki-type metric on $\text{T}_{(\mathbf{x}, P)} \text{Gr}_k(\text{T}\mathcal{M})$ is defined as*

$$\langle (\boldsymbol{\delta}, \Delta), (\tilde{\boldsymbol{\delta}}, \tilde{\Delta}) \rangle_{(\mathbf{x}, P)} := \langle \boldsymbol{\delta}, \tilde{\boldsymbol{\delta}} \rangle + \langle \Delta_{\mathbf{x}}, \tilde{\Delta}_{\mathbf{x}} \rangle, \quad \forall (\boldsymbol{\delta}, \Delta), (\tilde{\boldsymbol{\delta}}, \tilde{\Delta}) \in \text{T}_{(\mathbf{x}, P)} \text{Gr}_k(\text{T}\mathcal{M}),$$

where

$$\Delta_{\mathbf{x}} := \text{Proj}_{\text{T}_{\mathbf{x}}\mathcal{M}} \circ \Delta \circ \text{Proj}_{\text{T}_{\mathbf{x}}\mathcal{M}}, \quad \tilde{\Delta}_{\mathbf{x}} := \text{Proj}_{\text{T}_{\mathbf{x}}\mathcal{M}} \circ \tilde{\Delta} \circ \text{Proj}_{\text{T}_{\mathbf{x}}\mathcal{M}}. \quad (19)$$

Moreover, we denote the norm induced by the Sasaki-type metric with $\|\bullet\|_{(\mathbf{x}, P)}$. Then for any $(\boldsymbol{\delta}, \Delta) \in \text{T}_{(\mathbf{x}, P)} \text{Gr}_k(\text{T}\mathcal{M})$,

$$\|(\boldsymbol{\delta}, \Delta)\|_{(\mathbf{x}, P)} = (\|\boldsymbol{\delta}\|^2 + \|\Delta_{\mathbf{x}}\|^2)^{\frac{1}{2}}.$$

To preserve the feasibility condition in discretized algorithms, we need to define a retraction over $\text{Gr}_k(\text{T}\mathcal{M})$. One possible choice based on the retraction over \mathcal{M} is given in the following lemma.

Lemma 4 (Retraction over $\text{Gr}_k(\text{T}\mathcal{M})$). *Suppose that \mathcal{M} is a Riemannian submanifold of a Euclidean space \mathcal{E} with $\dim(\mathcal{M}) = d$ and $\text{Retr}^{\mathcal{M}} : \text{T}\mathcal{M} \rightarrow \mathcal{M}$ is a retraction over \mathcal{M} . Then $\text{Retr}^{\text{Gr}_k(\text{T}\mathcal{M})} : \text{T}(\text{Gr}_k(\text{T}\mathcal{M})) \rightarrow \text{Gr}_k(\text{T}\mathcal{M})$ defined as*

$$\text{Retr}_{(\mathbf{x}, P)}^{\text{Gr}_k(\text{T}\mathcal{M})}(\boldsymbol{\delta}, \Delta) := \left(\text{Retr}_{\mathbf{x}}^{\mathcal{M}}(\boldsymbol{\delta}), \text{Proj}_{\text{T}_{\text{Retr}_{\mathbf{x}}^{\mathcal{M}}(\boldsymbol{\delta})}\mathcal{M}} \circ \text{Exp}_P^{\text{Gr}_k(\text{T}_{\mathbf{x}}\mathcal{M})}(\Delta_{\mathbf{x}}) \circ \text{Proj}_{\text{T}_{\text{Retr}_{\mathbf{x}}^{\mathcal{M}}(\boldsymbol{\delta})}\mathcal{M}} \right), \quad (20)$$

for any $((\mathbf{x}, P), (\boldsymbol{\delta}, \Delta)) \in T(\text{Gr}_k(T\mathcal{M}))$, is a retraction over $\text{Gr}_k(T\mathcal{M})$, where $\Delta_{\mathbf{x}}$ is defined in Eq. (19). Its representative over $\text{St}_k(T\mathcal{M})$ is

$$\text{Retr}_{(\mathbf{x}, V)}^{\text{Gr}_k(T\mathcal{M})}(\boldsymbol{\delta}, \Delta V) := \left(\text{Retr}_{\mathbf{x}}^{\mathcal{M}}(\boldsymbol{\delta}), \text{Proj}_{T_{\text{Retr}_{\mathbf{x}}^{\mathcal{M}}(\boldsymbol{\delta})}\mathcal{M}}(VU \cos(\Sigma)U^\top + Q \sin(\Sigma)U^\top + VU_\perp U_\perp^\top) \right), \quad (21)$$

for any $((\mathbf{x}, V), (\boldsymbol{\delta}, \Delta V)) \in T(\text{St}_k(T\mathcal{M}))$ fulfilling $P = VV^\top$, where $Q \in \text{St}_r(\mathbb{R}^n)$, $\Sigma = \text{diag}(\sigma_1, \dots, \sigma_r) \in \mathbb{R}_{++}^{r \times r}$, and $U \in \text{St}_r(\mathbb{R}^k)$ satisfy $\Delta_{\mathbf{x}} V = Q\Sigma U^\top$, with $r \leq \min\{k, d - k\}$ the rank of $\Delta_{\mathbf{x}} V$, and $U_\perp \in \text{St}_{k-r}(\mathbb{R}^k)$ satisfies $U^\top U_\perp = 0$.

Proof. It is straightforward to verify that $\text{Retr}^{\text{Gr}_k(T\mathcal{M})}$ is smooth and $\text{Retr}_{(\mathbf{x}, P)}^{\text{Gr}_k(T\mathcal{M})}(0) = (\mathbf{x}, P)$. It then suffices to check its differential with respect to the second argument. By definition, for any $(\boldsymbol{\delta}, \Delta) \in T_{(\mathbf{x}, P)}(\text{Gr}_k(T\mathcal{M}))$,

$$\begin{aligned} & D\text{Retr}_{(\mathbf{x}, P)}^{\text{Gr}_k(T\mathcal{M})}(0)[(\boldsymbol{\delta}, \Delta)] \\ &= \lim_{s \rightarrow 0} \frac{1}{s} \left(\text{Retr}_{\mathbf{x}}^{\mathcal{M}}(s\boldsymbol{\delta}) - \mathbf{x}, \text{Proj}_{T_{\text{Retr}_{\mathbf{x}}^{\mathcal{M}}(s\boldsymbol{\delta})}\mathcal{M}} \circ \text{Exp}_P^{\text{Gr}_k(T_{\mathbf{x}}\mathcal{M})}(s\Delta_{\mathbf{x}}) \circ \text{Proj}_{T_{\text{Retr}_{\mathbf{x}}^{\mathcal{M}}(s\boldsymbol{\delta})}\mathcal{M}} - P \right). \end{aligned}$$

The limit of the first component is exactly $\boldsymbol{\delta}$ from the definition of retraction. For the second component, by the product rule and the fact that $P = \text{Proj}_{T_{\mathbf{x}}\mathcal{M}} \circ P \circ \text{Proj}_{T_{\mathbf{x}}\mathcal{M}}$,

$$\begin{aligned} & \lim_{s \rightarrow 0} \frac{1}{s} \left(\text{Proj}_{T_{\text{Retr}_{\mathbf{x}}^{\mathcal{M}}(s\boldsymbol{\delta})}\mathcal{M}} \circ \text{Exp}_P^{\text{Gr}_k(T_{\mathbf{x}}\mathcal{M})}(s\Delta_{\mathbf{x}}) \circ \text{Proj}_{T_{\text{Retr}_{\mathbf{x}}^{\mathcal{M}}(s\boldsymbol{\delta})}\mathcal{M}} - P \right) \\ &= \sum_{\ell=1}^k \Pi_{\mathbf{x}}(\boldsymbol{\delta}, \mathbf{v}_\ell) \mathbf{v}_\ell^\top + \text{Proj}_{T_{\mathbf{x}}\mathcal{M}} \circ \Delta \circ \text{Proj}_{T_{\mathbf{x}}\mathcal{M}} + \sum_{\ell=1}^k \mathbf{v}_\ell \Pi_{\mathbf{x}}(\boldsymbol{\delta}, \mathbf{v}_\ell)^\top \\ &= \text{Proj}_{T_{\mathbf{x}}\mathcal{M}} \circ \Delta \circ \text{Proj}_{T_{\mathbf{x}}\mathcal{M}} + \widehat{\Pi}_{\mathbf{x}}(\boldsymbol{\delta}, P) = \Delta, \end{aligned}$$

where the first equality is due to Eq. (10) and the property of retraction, the second equality uses the definition (16), and the last equality follows from the characterization (15). Consequently, $D\text{Retr}_{(\mathbf{x}, P)}^{\text{Gr}_k(T\mathcal{M})}(0)$ is an identity mapping on $T_{(\mathbf{x}, P)}(T\mathcal{M})$, as desired. The closed-form expression of the representative over $\text{St}_k(T\mathcal{M})$ can be readily derived in analogy to the proof of [11, Proposition 3.3]. \square

3.2 Constrained saddle dynamics on $\text{Gr}_k(T\mathcal{M})$

Equipped with the above geometrical tools of $\text{Gr}_k(T\mathcal{M})$, we are ready to develop the constrained saddle dynamics (CSD). Since $(\mathbf{x}(t), P(t)) \in \text{Gr}_k(T\mathcal{M})$ for any t , we require from Eq. (15) that

$$\frac{d\mathbf{x}}{dt}(t) \in T_{\mathbf{x}(t)}\mathcal{M}, \quad \frac{dP}{dt}(t) = \text{Proj}_{T_{\mathbf{x}(t)}\mathcal{M}} \circ \frac{dP}{dt}(t) \circ \text{Proj}_{T_{\mathbf{x}(t)}\mathcal{M}} + \widehat{\Pi}_{\mathbf{x}} \left(\frac{d\mathbf{x}}{dt}(t), P(t) \right) \quad (22)$$

hold for all the time, where $\widehat{\Pi}_{\mathbf{x}}$ is defined in Eq. (16). To achieve this, we set

$$\begin{aligned} \frac{d\mathbf{x}}{dt}(t) &:= -R_{\mathbf{x}(t), P(t)}(\text{grad}_{\mathcal{M}} f(\mathbf{x}(t))), \\ \frac{dP}{dt}(t) &:= -\text{Proj}_{T_{P(t)}\text{Gr}_k(T_{\mathbf{x}(t)}\mathcal{M})} \circ \text{Hess}_{\mathcal{M}} f(\mathbf{x}(t)) + \widehat{\Pi}_{\mathbf{x}(t)} \left(\frac{d\mathbf{x}}{dt}(t), P(t) \right), \end{aligned} \quad (23)$$

where $R_{\mathbf{x}(t), P(t)}$ is the reflection operator defined by $P(t)$ on $T_{\mathbf{x}(t)}\mathcal{M}$:

$$R_{\mathbf{x}(t), P(t)}(\mathbf{u}) := \mathbf{u} - 2P(t)\mathbf{u}, \quad \forall \mathbf{u} \in T_{\mathbf{x}(t)}\mathcal{M}, \quad (24)$$

and $\text{Proj}_{T_{P(t)}\text{Gr}_k(T_{\mathbf{x}(t)}\mathcal{M})}$ refers to the orthogonal projection operator onto the tangent space to $\text{Gr}_k(T_{\mathbf{x}(t)}\mathcal{M})$ at $P(t)$, which has a closed-form expression,

$$\text{Proj}_{T_{P(t)}\text{Gr}_k(T_{\mathbf{x}(t)}\mathcal{M})}(M) := [P(t), [P(t), M]], \quad (25)$$

for any symmetric bilinear form M over $T_{\mathbf{x}(t)}\mathcal{M}$. The \mathbf{x} -part is the same as in Eq. (5) except that we adopt the orthogonal projector. The first ingredient of the P -part is responsible for tracking the lowest k -dimensional invariant subspace of $\text{Hess}_{\mathcal{M}} f(\mathbf{x}(t))$ in $T_{\mathbf{x}(t)}\mathcal{M}$, following the Euler-Lagrange equation of the Rayleigh quotient minimization,

$$\min_{\tilde{P}} \text{Tr}(\tilde{P} \circ \text{Hess}_{\mathcal{M}} f(\mathbf{x}(t))), \quad \text{s. t. } \tilde{P} \in \text{Gr}_k(T_{\mathbf{x}(t)}\mathcal{M}),$$

while the second ingredient accounts for the changes in the tangent spaces, as explained in Section 2.2. The dynamics (23) can be horizontally lifted to one over $\text{St}_k(T\mathcal{M})$ as shown in Lemma 3:

$$\begin{aligned} \frac{d\mathbf{x}}{dt}(t) &:= -R_{\mathbf{x}(t), V(t)}(\text{grad}_{\mathcal{M}} f(\mathbf{x}(t))), \\ \frac{d\mathbf{v}_i}{dt}(t) &:= -\text{Proj}_{\mathbf{x}(t), V(t)^\perp}(\text{Hess}_{\mathcal{M}} f(\mathbf{x}(t))[\mathbf{v}_i(t)]) + \text{II}_{\mathbf{x}(t)}\left(\frac{d\mathbf{x}}{dt}(t), \mathbf{v}_i(t)\right), \\ i &= 1, \dots, k, \quad \text{with } V(t) := (\mathbf{v}_1(t), \dots, \mathbf{v}_k(t)). \end{aligned} \quad (26)$$

If the special manifolds (4) are considered, the second fundamental form in Eq. (26) recovers the third term of the right-hand side of Eq. (6). However, thanks to the explicit characterization of the tangent space to $\text{Gr}_k(T\mathcal{M})$ in Lemma 2, our methodology applies in more general settings since we only require the orthogonal projection onto the tangent space to define the second fundamental form. Some examples are listed as follows.

Example 1 (Second fundamental form in special cases).

- *Riemannian manifolds induced by global defining functions: $\mathcal{E} = \mathbb{R}^n$, \mathcal{M} is defined in Eq. (4). For any $\mathbf{x} \in \mathcal{M}$, we have*

$$\begin{aligned} T_{\mathbf{x}}\mathcal{M} &= \{\mathbf{v} \in \mathbb{R}^n \mid \text{grad } \mathbf{c}(\mathbf{x})\mathbf{v} = 0\}, \\ \text{Proj}_{T_{\mathbf{x}}\mathcal{M}}(\mathbf{v}) &= \left(I_n - \text{grad } \mathbf{c}(\mathbf{x})^\top (\text{grad } \mathbf{c}(\mathbf{x}) \cdot \text{grad } \mathbf{c}(\mathbf{x})^\top)^{-1} \text{grad } \mathbf{c}(\mathbf{x})\right) \mathbf{v} \end{aligned}$$

for any $\mathbf{v} \in \mathcal{E}$. Therefore, by Eq. (10), for any $\mathbf{u}, \mathbf{v} \in T_{\mathbf{x}}\mathcal{M}$,

$$\begin{aligned} \text{II}_{\mathbf{x}}(\mathbf{u}, \mathbf{v}) &= -(\text{Hess } \mathbf{c}(\mathbf{x})[\mathbf{u}])^\top \left(\text{grad } \mathbf{c}(\mathbf{x}) \cdot \text{grad } \mathbf{c}(\mathbf{x})^\top\right)^{-1} \text{grad } \mathbf{c}(\mathbf{x})\mathbf{v} \\ &\quad - \text{grad } \mathbf{c}(\mathbf{x})^\top \text{D} \left(\mathbf{y} \mapsto (\text{grad } \mathbf{c}(\mathbf{y}) \cdot \text{grad } \mathbf{c}(\mathbf{y})^\top)^{-1}\right) (\mathbf{x})[\mathbf{u}] \cdot \text{grad } \mathbf{c}(\mathbf{x})\mathbf{v} \\ &\quad - \text{grad } \mathbf{c}(\mathbf{x})^\top \left(\text{grad } \mathbf{c}(\mathbf{x}) \cdot \text{grad } \mathbf{c}(\mathbf{x})^\top\right)^{-1} (\text{Hess } \mathbf{c}(\mathbf{x})[\mathbf{u}]) \mathbf{v} \\ &= -\text{grad } \mathbf{c}(\mathbf{x})^\top \left(\text{grad } \mathbf{c}(\mathbf{x}) \cdot \text{grad } \mathbf{c}(\mathbf{x})^\top\right)^{-1} (\text{Hess } \mathbf{c}(\mathbf{x})[\mathbf{u}]) \mathbf{v}, \end{aligned}$$

where the last equality is due to $\text{grad } \mathbf{c}(\mathbf{x})\mathbf{v} = 0$. Notably, this recovers the third term on the right-hand side of Eq. (6) if we let $\mathbf{u} = \frac{d\mathbf{x}}{dt}(t)$. Some special cases fallen into this class and the corresponding second fundamental forms are listed as follows:

- *Flat space: $\mathcal{M} = \mathcal{E}$, $\text{II}_{\mathbf{x}} \equiv 0$.*
- *Sphere: $\mathcal{E} = \mathbb{R}^{d+1}$, $\mathcal{M} = \mathbb{S}^d$,*

$$\text{II}_{\mathbf{x}}(\mathbf{u}, \mathbf{v}) = -\langle \mathbf{u}, \mathbf{v} \rangle \mathbf{x}, \quad \forall \mathbf{x} \in \mathcal{M}, \mathbf{u}, \mathbf{v} \in T_{\mathbf{x}}\mathcal{M}.$$

- *Stiefel manifold: $\mathcal{E} = \mathbb{R}^{n \times p}$, $\mathcal{M} = \text{St}_p(\mathbb{R}^n)$,*

$$\text{II}_X(U, V) = -\frac{1}{2}X(U^\top V + V^\top U), \quad \forall X \in \text{St}_p(\mathbb{R}^n), U, V \in T_X\mathcal{M}.$$

- *Grassmann manifold:* $\mathcal{E} = \mathbb{R}_{\text{sym}}^{n \times n}$, $\mathcal{M} = \text{Gr}_p(\mathbb{R}^n)$. For any $P \in \mathcal{M}$, we have from [11] that

$$T_P \mathcal{M} = \left\{ \Gamma \in \mathbb{R}_{\text{sym}}^{n \times n} \mid \Gamma P + P\Gamma = \Gamma \right\}, \quad \text{Proj}_{T_P \mathcal{M}}(\Gamma) = [P, [P, \Gamma]], \quad \forall \Gamma \in \mathcal{E}.$$

Therefore, by Eq. (10), for any $\Gamma, \Delta \in T_P \mathcal{M}$,

$$\Pi_P(\Delta, \Gamma) = [\Delta, [P, \Gamma]] + [P, [\Delta, \Gamma]] = [\Delta, [P, \Gamma]].$$

The last equality is due to

$$\begin{aligned} [P, [\Delta, \Gamma]] &= [P, [\Delta P + P\Delta, \Gamma P + P\Gamma]] \\ &= [P, \Delta P\Gamma + P\Delta\Gamma P - \Gamma P\Delta - P\Gamma\Delta P] \\ &= P\Delta\Gamma P - P\Gamma\Delta P - P\Delta\Gamma P + P\Gamma\Delta P = 0, \end{aligned}$$

where we have used $\Gamma P + P\Gamma = \Gamma$, $\Delta P + P\Delta = \Delta$, $P\Gamma P = 0$, and $P\Delta P = 0$.

- *Fixed-rank manifold:* $\mathcal{E} = \mathbb{R}^{m \times n}$, $\mathcal{M} = \mathbb{R}_r^{m \times n}$. For any $X \in \mathcal{M}$, let $X = U\Sigma V^\top$ be its singular value decomposition, where $U \in \text{St}_r(\mathbb{R}^m)$, $\Sigma = \text{diag}(\sigma_1, \dots, \sigma_r) \in \mathbb{R}_{++}^{r \times r}$, and $V \in \text{St}_r(\mathbb{R}^n)$. We have from [13, Section 7.5] that

$$\begin{aligned} T_X \mathcal{M} &= \left\{ (U \ U_\perp) \begin{pmatrix} A & B \\ C & 0 \end{pmatrix} \begin{pmatrix} V^\top \\ V_\perp^\top \end{pmatrix} \mid A \in \mathbb{R}^{r \times r}, B \in \mathbb{R}^{r \times (n-r)}, C \in \mathbb{R}^{(m-r) \times r} \right\}, \\ \text{Proj}_{T_X \mathcal{M}}(Z) &= Z - (I_m - UU^\top)Z(I_n - VV^\top), \quad \forall Z \in \mathcal{E}. \end{aligned}$$

Note that for any smooth curve $c : \mathbb{R} \supseteq \mathcal{I} \rightarrow \mathcal{M}$ satisfying $X(0) = X$ and $X'(0) = \Psi \in T_X \mathcal{M}$, there exist smooth mappings $U(t) \in \text{St}_r(\mathbb{R}^m)$, $\Sigma(t) \in \mathbb{R}^{r \times r}$, and $V(t) \in \text{St}_r(\mathbb{R}^n)$ such that $X(t) = U(t)\Sigma(t)V(t)^\top$ and $U(0) = U$, $\Sigma(0) = \Sigma$, $V(0) = V$ hold in a small neighborhood of the origin. By the product rule,

$$U'(0)\Sigma V^\top + U\Sigma'(0)V^\top + U\Sigma V'(0)^\top = X'(0) = \Psi,$$

which yields

$$\Sigma'(0) = U^\top \Psi V, \quad U'(0) = (I_m - UU^\top)\Psi V \Sigma^{-1}, \quad V'(0) = (I_n - VV^\top)\Psi^\top U \Sigma^{-1}.$$

Therefore, by Eq. (10), for any $\Phi, \Psi \in T_X \mathcal{M}$,

$$\begin{aligned} \Pi_X(\Psi, \Phi) &= \left((I_m - UU^\top)\Psi V \Sigma^{-1} U^\top + U\Sigma^{-1} V^\top \Psi^\top (I_m - UU^\top) \right) \Phi (I_n - VV^\top) \\ &\quad + (I_m - UU^\top) \Phi \left((I_n - VV^\top) \Psi^\top U \Sigma^{-1} V^\top + V\Sigma^{-1} U^\top \Psi (I_n - VV^\top) \right) \\ &= (I_m - UU^\top) \left(\Psi V \Sigma^{-1} U^\top \Phi + \Phi V \Sigma^{-1} U^\top \Psi \right) (I_n - VV^\top), \end{aligned}$$

where the last equality is due to the fact that $(I_m - UU^\top)\Phi(I_n - VV^\top) = 0$.

We shall point out that the CSD (26) (or (23)) does not coincide completely with the existing dynamics in Eqs. (5) and (6). The difference consists in the tangent space component of V -dynamics: in the existing dynamics (6), the component is

$$-\text{Proj}_{\mathbf{x}(t), \mathbf{v}_i(t)^\perp} (\text{Hess}_{\mathcal{M}} f(\mathbf{x}(t))[\mathbf{v}_i(t)]) + 2 \sum_{j=1}^{i-1} \text{Proj}_{\mathbf{x}(t), \mathbf{v}_j(t)} (\text{Hess}_{\mathcal{M}} f(\mathbf{x}(t))[\mathbf{v}_i(t)]),$$

while in ours, the component reads

$$-\text{Proj}_{\mathbf{x}(t), \mathbf{v}_i(t)^\perp} (\text{Hess}_{\mathcal{M}} f(\mathbf{x}(t))[\mathbf{v}_i(t)]) + \sum_{j \neq i} \text{Proj}_{\mathbf{x}(t), \mathbf{v}_j(t)} (\text{Hess}_{\mathcal{M}} f(\mathbf{x}(t))[\mathbf{v}_i(t)]).$$

Algorithm 1 Discretized CSD over $\text{Gr}_k(\text{T}\mathcal{M})$.

Input: Initial point $(\mathbf{x}^{(0)}, P^{(0)}) \in \text{Gr}_k(\text{T}\mathcal{M})$, step size $\eta > 0$, maximum iteration number $\text{maxit} \in \mathbb{N}$, convergence tolerance $\text{tol} > 0$.

- 1: Set $t := 0$, $r_{\mathbf{x}}^{(0)} = r_P^{(0)} := \infty$.
- 2: **while** $t < \text{maxit}$ or $\max\{r_{\mathbf{x}}^{(t)}, r_P^{(t)}\} > \text{tol}$ **do**
- 3: Compute the \mathbf{x} -direction:

$$\mathbf{d}_{\mathbf{x}}^{(t)} := -R_{\mathbf{x}^{(t)}, P^{(t)}}(\text{grad}_{\mathcal{M}} f(\mathbf{x}^{(t)})) \in \text{T}_{\mathbf{x}^{(t)}} \mathcal{M}.$$

- 4: Compute the P -direction:

$$\mathbf{d}_P^{(t)} := -\text{Proj}_{\text{T}_{P^{(t)}} \text{Gr}_k(\text{T}_{\mathbf{x}^{(t)}} \mathcal{M})} \circ \text{Hess}_{\mathcal{M}} f(\mathbf{x}^{(t)}) \in \text{T}_{P^{(t)}} \text{Gr}_k(\text{T}_{\mathbf{x}^{(t)}} \mathcal{M}).$$

- 5: Update \mathbf{x} and P using the retraction defined in Eq. (20):

$$(\mathbf{x}^{(t+1)}, P^{(t+1)}) := \text{Retr}_{(\mathbf{x}^{(t)}, P^{(t)})}^{\text{Gr}_k(\text{T}\mathcal{M})}(\eta \mathbf{d}_{\mathbf{x}}^{(t)}, \eta \mathbf{d}_P^{(t)}) \in \text{Gr}_k(\text{T}\mathcal{M}).$$

- 6: **if** $t = 0$ **then**
- 7: Set $r_{\mathbf{x}}^{(t+1)} = r_P^{(t+1)} := 1$.
- 8: **else**
- 9: Update $r_{\mathbf{x}}^{(t+1)} := \|\mathbf{d}_{\mathbf{x}}^{(t)}\|/\|\mathbf{d}_{\mathbf{x}}^{(0)}\|$ and $r_P^{(t+1)} := \|\mathbf{d}_P^{(t)}\|/\|\mathbf{d}_P^{(0)}\|$.
- 10: **end if**
- 11: Set $t := t + 1$.
- 12: **end while**

Output: $(\mathbf{x}^{(t)}, P^{(t)}) \in \text{Gr}_k(\text{T}\mathcal{M})$.

The existing one is derived from the Lagrangian formalism combined with operator splitting [87], which is favorable due to its decoupled nature but does not respect the quotient structure (14). This can be problematic in theoretical analysis; see the discussions in Remark 1 later.

It is straightforward to verify that Eq. (22) holds if $(\mathbf{x}(t), P(t)) \in \text{Gr}_k(\text{T}\mathcal{M})$. Indeed, we are able to show the global well-definedness of the dynamics (23) if \mathcal{M} is compact.

Theorem 1 (Global well-definedness of the dynamics (23)). *Suppose that \mathcal{M} is a compact Riemannian submanifold of a Euclidean space \mathcal{E} with $\dim(\mathcal{M}) = d$. If $(\mathbf{x}(0), P(0)) \in \text{Gr}_k(\text{T}\mathcal{M})$, then the trajectory generated by the dynamics (23) always stays on $\text{Gr}_k(\text{T}\mathcal{M})$.*

Proof. Since \mathcal{M} is compact in \mathcal{E} , so is $\text{Gr}_k(\text{T}\mathcal{M})$ in its ambient space. The conclusion then follows directly from [47, Corollary 9.17]. \square

We then discretize the dynamics (23) by directly applying the forward Euler scheme and using the retraction (20), which yields Algorithm 1. Note that in step 4, we do not compute the term involving the second fundamental form. This is credited to the construction of the retraction (20), in which the normal component makes no difference. In light of the quotient structure (14), we can also obtain a representative version running over $\text{St}_k(\text{T}\mathcal{M})$ by horizontal lifts; see Algorithm 2. In comparison with Algorithm 1, Algorithm 2 can be more computationally economic.

4 Theoretical analysis

In this section, we analyze the linear stability of the dynamics (23) and the local convergence of Algorithm 1.

Algorithm 2 Discretized CSD using representatives over $\text{St}_k(\text{T}\mathcal{M})$.

Input: Initial point $(\mathbf{x}^{(0)}, V^{(0)}) \in \text{St}_k(\text{T}\mathcal{M})$, step size $\eta > 0$, maximum iteration number $maxit \in \mathbb{N}$, convergence tolerance $tol > 0$.

- 1: Set $t := 0$, $r_{\mathbf{x}}^{(0)} = r_V^{(0)} := \infty$.
- 2: **while** $t < maxit$ or $\max\{r_{\mathbf{x}}^{(t)}, r_V^{(t)}\} > tol$ **do**
- 3: Compute the \mathbf{x} -direction:

$$\mathbf{d}_{\mathbf{x}}^{(t)} := -R_{\mathbf{x}^{(t)}, V^{(t)}}(\text{grad}_{\mathcal{M}} f(\mathbf{x}^{(t)})) \in \text{T}_{\mathbf{x}^{(t)}} \mathcal{M}.$$

- 4: Compute the V -direction:

$$\mathbf{d}_{\mathbf{v}_i}^{(t)} := -\text{Proj}_{\mathbf{x}^{(t)}, (V^{(t)})^\perp}(\text{Hess}_{\mathcal{M}} f(\mathbf{x}^{(t)})[\mathbf{v}_i^{(t)}]) \in \text{T}_{\mathbf{x}^{(t)}} \mathcal{M}, \quad i = 1, \dots, k,$$

and set $\mathbf{d}_V^{(t)} := (\mathbf{d}_{\mathbf{v}_1}^{(t)}, \dots, \mathbf{d}_{\mathbf{v}_k}^{(t)}) \in \text{T}_{V^{(t)}} \text{St}_k(\text{T}_{\mathbf{x}^{(t)}} \mathcal{M})$.

- 5: Update \mathbf{x} and V using the retraction defined in Eq. (21):

$$(\mathbf{x}^{(t+1)}, V^{(t+1)}) := \text{Retr}_{(\mathbf{x}^{(t)}, V^{(t)})}^{\text{Gr}_k(\text{T}\mathcal{M})}(\eta \mathbf{d}_{\mathbf{x}}^{(t)}, \eta \mathbf{d}_V^{(t)}) \in \text{St}_k(\text{T}\mathcal{M}).$$

- 6: **if** $t = 0$ **then**
- 7: Set $r_{\mathbf{x}}^{(t+1)} = r_V^{(t+1)} := 1$.
- 8: **else**
- 9: Update $r_{\mathbf{x}}^{(t+1)} := \|\mathbf{d}_{\mathbf{x}}^{(t)}\|/\|\mathbf{d}_{\mathbf{x}}^{(0)}\|$ and $r_V^{(t+1)} := \|\mathbf{d}_V^{(t)}\|/\|\mathbf{d}_V^{(0)}\|$.
- 10: **end if**
- 11: Set $t := t + 1$.
- 12: **end while**

Output: $(\mathbf{x}^{(t)}, V^{(t)}) \in \text{St}_k(\text{T}\mathcal{M})$.

4.1 Linear stability analysis of the dynamics

Let $\mathbf{w} := (\mathbf{x}, P) \in \text{Gr}_k(\text{T}\mathcal{M})$ and $\mathbf{h} : \text{Gr}_k(\text{T}\mathcal{M}) \rightarrow \text{T}(\text{Gr}_k(\text{T}\mathcal{M}))$ be the vector field defined as $\mathbf{h}(\mathbf{w}) := (h_1(\mathbf{w}), h_2(\mathbf{w}))$, where

$$\begin{aligned} h_1(\mathbf{w}) &:= -R_{\mathbf{w}}(\text{grad}_{\mathcal{M}} f(\mathbf{x})), \\ h_2(\mathbf{w}) &:= -\text{Proj}_{\text{T}_P \text{Gr}_k(\text{T}_{\mathbf{x}} \mathcal{M})} \circ \text{Hess}_{\mathcal{M}} f(\mathbf{x}) + \widehat{\text{II}}_{\mathbf{x}}(h_1(\mathbf{w}), P). \end{aligned} \tag{27}$$

Note that $R_{\mathbf{w}}$ should be identified as the one in Eq. (24). It follows that, Eq. (23) can be rewritten compactly as the following dynamics over $\text{Gr}_k(\text{T}\mathcal{M})$:

$$\frac{d\mathbf{w}}{dt}(t) = \mathbf{h}(\mathbf{w}(t)), \tag{28}$$

with the initial condition $\mathbf{w}(0) = (\mathbf{x}(0), P(0)) \in \text{Gr}_k(\text{T}\mathcal{M})$.

In the following, we aim to establish the linear stability of the dynamics (28) using the geometrical tools for $\text{Gr}_k(\text{T}\mathcal{M})$ in Section 3.1. Before that, we first figure out the expression of the differential $D\mathbf{h}(\mathbf{w})$.

Lemma 5 (Differential of \mathbf{h}). *Suppose that f is C^3 , \mathcal{M} is a Riemannian submanifold of a Euclidean space \mathcal{E} with $\dim(\mathcal{M}) = d$, and $\mathbf{h} : \text{Gr}_k(\text{T}\mathcal{M}) \rightarrow \text{T}(\text{Gr}_k(\text{T}\mathcal{M}))$ is the vector field over $\text{Gr}_k(\text{T}\mathcal{M})$ defined in Eq. (27). Then for any $\mathbf{w} := (\mathbf{x}, P) \in \text{Gr}_k(\text{T}\mathcal{M})$ and $D := (\delta, \Delta) \in \text{T}_{\mathbf{w}}(\text{Gr}_k(\text{T}\mathcal{M}))$, it holds that*

$$Dh_1(\mathbf{w})[D] = -R_{\mathbf{w}}(\text{Hess}_{\mathcal{M}} f(\mathbf{x})[\delta]) + \mathbf{m}_1(\mathbf{w})[\delta] + \mathbf{m}_2(\mathbf{w})[\Delta],$$

$$Dh_2(\mathbf{w})[D] = -[\Delta, [P, \text{Hess}_{\mathcal{M}} f(\mathbf{x})]] - [P, [\Delta, \text{Hess}_{\mathcal{M}} f(\mathbf{x})]] + \mathbf{m}_3(\mathbf{w})[\delta] + \mathbf{m}_4(\mathbf{w})[\Delta],$$

where

$$\begin{aligned}
\mathbf{m}_1(\mathbf{w})[\delta] &:= -D(\mathbf{y} \mapsto O_{\mathbf{y}, P}^R)(\mathbf{x})[\delta](\text{grad}_{\mathcal{M}} f(\mathbf{x})) - O_{\mathbf{w}}^R(\Pi_{\mathbf{x}}(\delta, \text{grad}_{\mathcal{M}} f(\mathbf{x}))), \\
\mathbf{m}_2(\mathbf{w})[\Delta] &:= -D(Q \mapsto O_{\mathbf{x}, Q}^R)(P)[\Delta](\text{grad}_{\mathcal{M}} f(\mathbf{x})), \\
\mathbf{m}_3(\mathbf{w})[\delta] &:= -D(\mathbf{y} \mapsto O_{\mathbf{y}, P}^{\text{Proj}})(\mathbf{x})[\delta] \circ \text{Hess}_{\mathcal{M}} f(\mathbf{x}) - O_{\mathbf{w}}^{\text{Proj}} \circ D\bar{H}(\mathbf{x})[\delta] \\
&\quad + D(\mathbf{y} \mapsto O_{\mathbf{y}}^{\hat{\Pi}})(\mathbf{x})[\delta](h_1(\mathbf{w}), P) + O_{\mathbf{x}}^{\hat{\Pi}}(D(\mathbf{y} \mapsto h_1(\mathbf{y}, P))(\mathbf{x})[\delta], P), \\
\mathbf{m}_4(\mathbf{w})[\Delta] &:= O_{\mathbf{x}}^{\hat{\Pi}}(D(Q \mapsto h_1(\mathbf{x}, Q))(P)[\Delta], P) + O_{\mathbf{x}}^{\hat{\Pi}}(h_1(\mathbf{w}), \Delta),
\end{aligned}$$

$(\mathbf{x}, P) \mapsto O_{\mathbf{x}, P}^R$, $(\mathbf{x}, P) \mapsto O_{\mathbf{x}, P}^{\text{Proj}}$, $\mathbf{x} \mapsto O_{\mathbf{x}}^{\hat{\Pi}}$, and \bar{H} are any smooth extensions of $(\mathbf{x}, P) \mapsto R_{\mathbf{x}, P}$, $(\mathbf{x}, P) \mapsto \text{Proj}_{T_P \text{Gr}_k(T_{\mathbf{x}} \mathcal{M})}$, $\mathbf{x} \mapsto \hat{\Pi}_{\mathbf{x}}$, and $\text{Hess}_{\mathcal{M}} f$ to proper ambient spaces, respectively.

Proof. Let $c : \mathbb{R} \supseteq \mathcal{I} \rightarrow \text{Gr}_k(T\mathcal{M})$ be a smooth curve over $\text{Gr}_k(T\mathcal{M})$ such that $c(0) = \mathbf{w}$ and $c'(0) = D$. We thus have

$$D\mathbf{h}(\mathbf{w})[D] = (\mathbf{h} \circ c)'(0) = ((h_1 \circ c)'(0), (h_2 \circ c)'(0)).$$

By the product and chain rules,

$$\begin{aligned}
(h_1 \circ c)'(0) &= \lim_{s \rightarrow 0} (h_1(c(s)) - h_1(c(0))) / s \\
&= - (D(\mathbf{y} \mapsto O_{\mathbf{y}, P}^R)(\mathbf{x})[\delta] + D(Q \mapsto O_{\mathbf{x}, Q}^R)(P)[\Delta])(\text{grad}_{\mathcal{M}} f(\mathbf{x})) \\
&\quad - O_{\mathbf{w}}^R(P_{\mathbf{x}, \delta}(\text{grad } f(\mathbf{x})) + \text{Proj}_{T_{\mathbf{x}} \mathcal{M}}(\text{Hess } f(\mathbf{x})[\delta])) \\
&= - (D(\mathbf{y} \mapsto O_{\mathbf{y}, P}^R)(\mathbf{x})[\delta] + D(Q \mapsto O_{\mathbf{x}, Q}^R)(P)[\Delta])(\text{grad}_{\mathcal{M}} f(\mathbf{x})) \\
&\quad - O_{\mathbf{w}}^R(\text{Hess}_{\mathcal{M}} f(\mathbf{x})[\delta] + \Pi_{\mathbf{x}}(\delta, \text{grad}_{\mathcal{M}} f(\mathbf{x}))) \\
&= - R_{\mathbf{w}}(\text{Hess}_{\mathcal{M}} f(\mathbf{x})[\delta]) + \mathbf{m}_1(\mathbf{w})[\delta] + \mathbf{m}_2(\mathbf{w})[\Delta],
\end{aligned}$$

where the second equality uses Eqs. (9) and (11), and

$$\begin{aligned}
(h_2 \circ c)'(0) &= \lim_{s \rightarrow 0} (h_2(c(s)) - h_2(c(0))) / s \\
&= - D(\mathbf{y} \mapsto O_{\mathbf{y}, P}^{\text{Proj}})(\mathbf{x})[\delta] \circ \text{Hess}_{\mathcal{M}} f(\mathbf{x}) - O_{\mathbf{w}}^{\text{Proj}} \circ D\bar{H}(\mathbf{x})[\delta] \\
&\quad + D(\mathbf{y} \mapsto O_{\mathbf{y}}^{\hat{\Pi}})(\mathbf{x})[\delta](h_1(\mathbf{w}), P) + O_{\mathbf{x}}^{\hat{\Pi}}(D(\mathbf{y} \mapsto h_1(\mathbf{y}, P))(\mathbf{x})[\delta], P) \\
&\quad - D(Q \mapsto O_{\mathbf{x}, Q}^{\text{Proj}})(P)[\Delta] \circ \text{Hess}_{\mathcal{M}} f(\mathbf{x}) + O_{\mathbf{x}}^{\hat{\Pi}}(h_1(\mathbf{w}), \Delta) \\
&\quad + O_{\mathbf{x}}^{\hat{\Pi}}(D(Q \mapsto h_1(\mathbf{x}, Q))(P)[\Delta], P) \\
&= - [\Delta, [P, \text{Hess}_{\mathcal{M}} f(\mathbf{x})]] - [P, [\Delta, \text{Hess}_{\mathcal{M}} f(\mathbf{x})]] + \mathbf{m}_3(\mathbf{w})[\delta] + \mathbf{m}_4(\mathbf{w})[\Delta],
\end{aligned}$$

where the last equality follows from Eq. (25). The proof is complete. \square

Theorem 2 (Linear stability of the dynamics (28)). *Suppose that f is C^3 , \mathcal{M} is a Riemannian submanifold of a Euclidean space \mathcal{E} with $\dim(\mathcal{M}) = d$, $\mathbf{w}^* := (\mathbf{x}^*, P^*) \in \text{Gr}_k(T\mathcal{M})$, and $\text{Hess}_{\mathcal{M}} f(\mathbf{x}^*)$ is nondegenerate, whose eigenvalues are $\lambda_1^* \leq \dots \leq \lambda_k^* < \lambda_{k+1}^* \leq \dots \leq \lambda_d^*$. Then \mathbf{w}^* is a linearly steady state of the dynamics (28) if and only if \mathbf{x}^* is an index- k constrained SP of f over \mathcal{M} and P^* is an orthogonal projector onto the lowest k -dimensional invariant subspace of $\text{Hess}_{\mathcal{M}} f(\mathbf{x}^*)$.*

Proof. The proof revolves around the spectrum of $D\mathbf{h}(\mathbf{w}^*)$.

Necessity. Suppose that \mathbf{w}^* is a linearly steady state of dynamics (28). Therefore, $d\mathbf{w} / dt$ vanishes at \mathbf{w}^* , which implies that

- $\text{grad}_{\mathcal{M}} f(\mathbf{x}^*) = 0$, i.e., \mathbf{x}^* is a critical point of f over \mathcal{M} . This further yields $\mathbf{m}_1(\mathbf{w}^*) = 0$, $\mathbf{m}_2(\mathbf{w}^*) = 0$, and $\mathbf{m}_4(\mathbf{w}^*) = 0$ from their definitions in Lemma 5;
- $[P^*, [P^*, \text{Hess}_{\mathcal{M}} f(\mathbf{x}^*)]] = 0$, i.e., P^* is an orthogonal projector onto a k -dimensional invariant subspace of $\text{Hess}_{\mathcal{M}} f(\mathbf{x}^*)$.

The differential $D\mathbf{h}(\mathbf{w}^*)[D]$ in Lemma 5 thus simplifies to

$$D\mathbf{h}(\mathbf{w}^*)[D] = \begin{pmatrix} -R_{\mathbf{w}^*}(\text{Hess}_{\mathcal{M}} f(\mathbf{x}^*)[\delta]) \\ -[P^*, [\Delta, \text{Hess}_{\mathcal{M}} f(\mathbf{x}^*)]] + \mathbf{m}_3(\mathbf{w}^*)[\delta] \end{pmatrix}. \quad (29)$$

Moreover, since $\pi^{\text{Gr}_k(\text{T}\mathcal{M})} \circ \mathbf{h} = \text{Id}_{\text{Gr}_k(\text{T}\mathcal{M})}$, where $\pi^{\text{Gr}_k(\text{T}\mathcal{M})} : \text{T}(\text{Gr}_k(\text{T}\mathcal{M})) \rightarrow \text{Gr}_k(\text{T}\mathcal{M})$ is defined as $\pi^{\text{Gr}_k(\text{T}\mathcal{M})}(\mathbf{w}, D) = \mathbf{w}$ for any $(\mathbf{w}, D) \in \text{T}(\text{Gr}_k(\text{T}\mathcal{M}))$, we have by the chain rule that

$$D\pi^{\text{Gr}_k(\text{T}\mathcal{M})}(\mathbf{h}(\mathbf{w}))[D\mathbf{h}(\mathbf{w})] = 0, \quad \forall \mathbf{w} \in \text{Gr}_k(\text{T}\mathcal{M}).$$

That is to say, the range of $D\mathbf{h}(\mathbf{w})$ is included in the vertical subspace of $\text{T}_{\mathbf{h}(\mathbf{w})}(\text{T}(\text{Gr}_k(\text{T}\mathcal{M})))$ induced by $\pi^{\text{Gr}_k(\text{T}\mathcal{M})}$, which is isomorphic to $\text{T}_{\mathbf{w}}(\text{Gr}_k(\text{T}\mathcal{M}))$. It follows that, we could regard $D\mathbf{h}(\mathbf{w})$ as a mapping from $\text{T}_{\mathbf{w}}(\text{Gr}_k(\text{T}\mathcal{M}))$ to itself.

By the Hartman-Grobman linearization theorem [3], the linear stability of \mathbf{w}^* implies that all of the eigenvalues of $D\mathbf{h}(\mathbf{w}^*)$ have negative real parts. By Lemma 2, these eigenvalues coincide with those of $B^{-1/2}AB^{-1/2}$, where $A \in \mathbb{R}^{\hat{d} \times \hat{d}}$ and $B \in \mathbb{R}_{\text{sym}}^{\hat{d} \times \hat{d}}$ (with $\hat{d} := d + k(d - k)$) are defined respectively using the Sasaki-type metric in Definition 1 as

$$\begin{aligned} A_{q,q'} &:= \langle D_{q'}^*, D\mathbf{h}(\mathbf{w}^*)[D_q^*] \rangle_{\mathbf{w}^*}, & B_{q,q'} &:= \langle D_{q'}^*, D_q^* \rangle_{\mathbf{w}^*}, \\ A_{ij,i'j'} &:= \langle D_{i'j'}^*, D\mathbf{h}(\mathbf{w}^*)[D_{ij}^*] \rangle_{\mathbf{w}^*}, & B_{ij,i'j'} &:= \langle D_{i'j'}^*, D_{ij}^* \rangle_{\mathbf{w}^*} \end{aligned}$$

with

$$\begin{aligned} D_q^* &:= (\delta_q^*, \Delta_q^*) := \left(\mathbf{v}_q^*, \widehat{\Pi}_{\mathbf{x}^*}(\mathbf{v}_q^*, P^*) \right), \quad q = 1, \dots, d, \\ D_{ij}^* &:= (\delta_{ij}^*, \Delta_{ij}^*) := \left(0, \frac{1}{\sqrt{2}}(\mathbf{v}_i^*(\mathbf{v}_j^*)^\top + \mathbf{v}_j^*(\mathbf{v}_i^*)^\top) \right), \quad i = 1, \dots, k, \quad j = k + 1, \dots, d. \end{aligned}$$

Here, $\{(\mu_q^*, \mathbf{v}_q^*)\}_{q=1}^d$ are the eigenpairs of $\text{Hess}_{\mathcal{M}} f(\mathbf{x}^*)$ such that $P^* = \sum_{\ell=1}^k \mathbf{v}_\ell^* (\mathbf{v}_\ell^*)^\top$. Indeed, by Definition 1 and Eq. (29) and noticing that $\{D_q^*\}_{q=1}^d$ and $\{D_{ij}^*\}_{\substack{i=1, \dots, k \\ j=k+1, \dots, d}}^d$ respectively span the horizontal and vertical subspaces of $\text{T}_{\mathbf{w}^*}(\text{Gr}_k(\text{T}\mathcal{M}))$ (see Lemma 3), we could work out the entries in A and B explicitly:

$$A_{q,q'} = \begin{cases} \mu_q^* \delta_{q,q'}, & q, q' = 1, \dots, k, \\ -\mu_q^* \delta_{q,q'}, & q, q' = k + 1, \dots, d, \\ 0, & \text{otherwise,} \end{cases}$$

$$A_{q,ij} = 0, \quad q = 1, \dots, d, \quad i = 1, \dots, k, \quad j = k + 1, \dots, d,$$

$$A_{ij,q} = \langle \Delta_{ij}^*, \mathbf{m}_3(\mathbf{w}^*)[\mathbf{v}_q^*] \rangle, \quad q = 1, \dots, d, \quad i = 1, \dots, k, \quad j = k + 1, \dots, d,$$

$$A_{ij,i'j'} = (\mu_i^* - \mu_j^*) \delta_{i,i'} \delta_{j,j'}, \quad i, i' = 1, \dots, k, \quad j, j' = k + 1, \dots, d,$$

and

$$B_{q,q'} = \delta_{q,q'}, \quad q, q' = 1, \dots, d; \quad B_{ij,i'j'} = \delta_{i,i'} \delta_{j,j'}, \quad i, i' = 1, \dots, k, \quad j, j' = k + 1, \dots, d.$$

Consequently, $B^{-1/2}AB^{-1/2}$ is lower (or upper) triangular and its eigenvalues are exactly

$$\{\mu_q^*\}_{q=1}^k, \quad \{-\mu_q^*\}_{q=k+1}^d, \quad \text{and} \quad \{\mu_i^* - \mu_j^*\}_{\substack{i=1, \dots, k \\ j=k+1, \dots, d}}.$$

Since they are all negative, we get $\max\{\mu_1^*, \dots, \mu_k^*\} < 0 < \min\{\mu_{k+1}^*, \dots, \mu_d^*\}$. This indicates that \mathbf{x}^* is an index- k constrained SP of f over \mathcal{M} , P^* is an orthogonal projector onto the lowest k -dimensional invariant subspace of $\text{Hess}_{\mathcal{M}} f(\mathbf{x}^*)$, and $\{\mu_1^*, \dots, \mu_k^*\} = \{\lambda_1^*, \dots, \lambda_k^*\}$, as desired.

Sufficiency. Suppose that \mathbf{x}^* is an index- k constrained SP of f over \mathcal{M} and P^* is an orthogonal projector onto the lowest k -dimensional invariant subspace of $\text{Hess}_{\mathcal{M}} f(\mathbf{x}^*)$. Therefore, $\text{grad}_{\mathcal{M}} f(\mathbf{x}^*) = 0$ and $\lambda_1^* \leq \dots \leq \lambda_k^* < 0 < \lambda_{k+1}^* \leq \dots \leq \lambda_d^*$. By similar arguments as above, we could obtain that the eigenvalues of $\mathbf{D}\mathbf{h}(\mathbf{w}^*)$ are exactly

$$\{\lambda_q^*\}_{q=1}^k, \quad \{-\lambda_q^*\}_{q=k+1}^d, \quad \text{and} \quad \{\lambda_i^* - \lambda_j^*\}_{\substack{i=1, \dots, k \\ j=k+1, \dots, d}}^i,$$

which are all negative, implying that $\mathbf{w}^* = (\mathbf{x}^*, P^*)$ is linearly steady. \square

Remark 1. In comparison with the linear stability results in the existing work [87, Theorem 1], Theorem 2 not only sits in more general manifold settings, but also requires weaker assumptions on the eigenvalues of Riemannian Hessian. More specifically, we only ask for a positive gap between λ_k^* and λ_{k+1}^* , whereas the existing one assumes additionally that $\{\lambda_i^*\}_{i=1}^k$ are all simple (cf. [87, Eqs. (34) and (40)]). This advantage is due to the fact that we respect the intrinsic quotient structure (14) by introducing the Grassmann bundle $\text{Gr}_k(\text{T}\mathcal{M})$.

4.2 Local convergence analysis of the discretized algorithm

In what follows, we show the local convergence properties of Algorithm 1.

Lemma 6. Suppose that \mathcal{N} is a Riemannian submanifold of a Euclidean space, $\text{Retr}^{\mathcal{N}} : \text{T}\mathcal{N} \rightarrow \mathcal{N}$ is a retraction over \mathcal{N} , and $\mathbf{y} \in \mathcal{N}$. Then there exist constants $c_1 > 0$ and $r_1 > 0$ such that the following two statements hold at the same time:

- $\text{Exp}_{\mathbf{y}}^{\mathcal{N}} : \text{T}_{\mathbf{y}}\mathcal{N} \rightarrow \mathcal{N}$ is a diffeomorphism between $\mathcal{B}_{\mathbf{y}}(0, r_1) := \{\mathbf{u} \in \text{T}_{\mathbf{y}}\mathcal{N} \mid \|\mathbf{u}\| < r_1\}$ and $\mathcal{U} := \text{Exp}_{\mathbf{y}}^{\mathcal{N}}(\mathcal{B}_{\mathbf{y}}(0, r_1))$.
- The inequality $\text{dist}_{\mathcal{N}}(\mathbf{y}', \text{Retr}_{\mathbf{y}'}^{\mathcal{N}}(\mathbf{u}')) \leq c_1 \|\mathbf{u}'\|$ holds for any $\mathbf{y}' \in \text{Exp}_{\mathbf{y}}(\text{cl}(\mathcal{B}_{\mathbf{y}}(0, r_1)))$ and $\mathbf{u}' \in \text{T}_{\mathbf{y}'}\mathcal{N}$ with $\|\mathbf{u}'\| \leq r_1$. In particular, if $\text{Retr}^{\mathcal{N}} = \text{Exp}^{\mathcal{N}}$, then the equality holds with $c_1 = 1$.

Proof. For the first statement, it suffices to note $\text{DExp}_{\mathbf{y}}^{\mathcal{N}}(0) = \text{Id}_{\text{T}_{\mathbf{y}}\mathcal{N}}$ and then use the implicit function theorem. For the second one, please refer to [13, Lemma 6.32 and Proposition 10.22]. \square

Lemma 7 (Residual after single iteration). Suppose that f is C^3 , \mathcal{M} is a Riemannian submanifold of a Euclidean space \mathcal{E} with $\dim(\mathcal{M}) = d$, $\mathbf{x}^* \in \mathcal{M}$ is an index- k constrained SP of f over \mathcal{M} , $\text{Hess}_{\mathcal{M}} f(\mathbf{x}^*)$ is nondegenerate, whose eigenvalues are $\lambda_1^* \leq \dots \leq \lambda_k^* < \lambda_{k+1}^* \leq \dots \leq \lambda_d^*$, and $P^* \in \text{Gr}_k(\text{T}_{\mathbf{x}^*}\mathcal{M})$ is an orthogonal projector onto the lowest k -dimensional invariant subspace of $\text{Hess}_{\mathcal{M}} f(\mathbf{x}^*)$. Let $\mathbf{w}^* := (\mathbf{x}^*, P^*) \in \text{Gr}_k(\text{T}\mathcal{M})$. Consider the following iterative mapping $F : \text{T}_{\mathbf{w}^*}(\text{Gr}_k(\text{T}\mathcal{M})) \rightarrow \text{T}_{\mathbf{w}^*}(\text{Gr}_k(\text{T}\mathcal{M}))$ defined as

$$F(D) := \left(\text{Exp}_{\mathbf{w}^*}^{\text{Gr}_k(\text{T}\mathcal{M})} \right)^{-1} \left(\text{Retr}_{\tilde{\mathbf{w}}(D)}^{\text{Gr}_k(\text{T}\mathcal{M})}(\eta \cdot \mathbf{h}(\tilde{\mathbf{w}}(D))) \right) =: (F_1(D), F_2(D)), \quad (30)$$

for any $D := (\delta, \Delta) \in \text{T}_{\mathbf{w}^*}(\text{Gr}_k(\text{T}\mathcal{M}))$, where $\tilde{\mathbf{w}}(D) := \text{Exp}_{\mathbf{w}^*}^{\text{Gr}_k(\text{T}\mathcal{M})}(D) \in \text{Gr}_k(\text{T}\mathcal{M})$, and η is a step size satisfying

$$0 < \eta < \frac{\min\{(r_1 - r_2)/c_1, r_1\}}{\sup_{\|D\|_{\mathbf{w}^*} \leq r_1} \|\mathbf{h}(\tilde{\mathbf{w}}(D))\|_{\mathbf{w}^*}}, \quad (31)$$

with c_1 and r_1 the constants in Lemma 6 (associated to $\mathcal{N} = \text{Gr}_k(\text{T}\mathcal{M})$, $\text{Retr}^{\mathcal{N}} = \text{Retr}^{\text{Gr}_k(\text{T}\mathcal{M})}$ or $\text{Exp}^{\text{Gr}_k(\text{T}\mathcal{M})}$, and $\mathbf{y} = \mathbf{w}^*$) and $r_2 \in (0, r_1)$. Then F is well-defined and smooth over the

subset $\{D \in \mathrm{T}_{\mathbf{w}^*}(\mathrm{Gr}_k(\mathrm{T}\mathcal{M})) : \|D\|_{\mathbf{w}^*} < r_2\}$. Moreover, there exist constants $r_3 \in (0, r_2]$ and $c_3 \geq 0$ such that

$$\begin{pmatrix} \|F_1(D)\| \\ \|F_2(D)_{\mathbf{x}^*}\| \end{pmatrix} \leq A(\eta) \begin{pmatrix} \|\delta\| \\ \|\Delta_{\mathbf{x}^*}\| \end{pmatrix} \quad (32)$$

holds over the subset $\{D \in \mathrm{T}_{\mathbf{w}^*}(\mathrm{Gr}_k(\mathrm{T}\mathcal{M})) : \|D\|_{\mathbf{w}^*} < r_3\}$, where

$$A(\eta) := \begin{pmatrix} q_1(\eta) + c_3 r_3 & c_3 r_3 \\ \eta M + c_3 r_3 & q_2(\eta) + c_3 r_3 \end{pmatrix},$$

$F_2(D)_{\mathbf{x}^*}$ and $\mathbf{m}_3(\mathbf{w}^*)_{\mathbf{x}^*}$ are defined similarly as in Eq. (19), $M := \|\mathbf{m}_3(\mathbf{w}^*)_{\mathbf{x}^*}\|$, and

$$\begin{aligned} q_1(\eta) &:= \max \{ |1 - \eta \lambda_{\min}^*|, |1 - \eta \lambda_{\max}^*| \}, \quad q_2(\eta) := \max \{ |1 - \eta \Delta \lambda_{k+1,k}^*|, |1 - \eta \Delta \lambda_{d1}^*| \}, \\ \lambda_{\min}^* &:= \min_{i=1}^d |\lambda_i^*|, \quad \lambda_{\max}^* := \max_{i=1}^d |\lambda_i^*|, \quad \Delta \lambda_{ji}^* := \lambda_j^* - \lambda_i^*, \quad i = 1, \dots, k, \quad j = k+1, \dots, d. \end{aligned}$$

Proof. We first show the well-definedness of F , i.e., the Riemannian distance between \mathbf{w}^* and $\mathrm{Retr}_{\tilde{\mathbf{w}}(D)}^{\mathrm{Gr}_k(\mathrm{T}\mathcal{M})}(\eta \cdot \mathbf{h}(\tilde{\mathbf{w}}(D)))$ falls below r_1 . By the triangle inequality of the Riemannian distance,

$$\begin{aligned} &\mathrm{dist}_{\mathrm{Gr}_k(\mathrm{T}\mathcal{M})} \left(\mathbf{w}^*, \mathrm{Retr}_{\tilde{\mathbf{w}}(D)}^{\mathrm{Gr}_k(\mathrm{T}\mathcal{M})}(\eta \cdot \mathbf{h}(\tilde{\mathbf{w}}(D))) \right) \\ &\leq \mathrm{dist}_{\mathrm{Gr}_k(\mathrm{T}\mathcal{M})}(\mathbf{w}^*, \tilde{\mathbf{w}}(D)) + \mathrm{dist}_{\mathrm{Gr}_k(\mathrm{T}\mathcal{M})} \left(\tilde{\mathbf{w}}(D), \mathrm{Retr}_{\tilde{\mathbf{w}}(D)}^{\mathrm{Gr}_k(\mathrm{T}\mathcal{M})}(\eta \cdot \mathbf{h}(\tilde{\mathbf{w}}(D))) \right) \\ &\leq \|D\|_{\mathbf{w}^*} + c_1 \eta \|\mathbf{h}(\tilde{\mathbf{w}}(D))\|_{\mathbf{w}^*} \leq r_2 + c_1 \eta \sup_{\|D\|_{\mathbf{w}^*} \leq r_1} \|\mathbf{h}(\tilde{\mathbf{w}}(D))\|_{\mathbf{w}^*} < r_1, \end{aligned}$$

where the second inequality leverages Lemma 6, the fact that $\|D\|_{\mathbf{w}^*} < r_2 < r_1$, and the assumption (31) on η , in that

$$\eta \|\mathbf{h}(\tilde{\mathbf{w}}(D))\|_{\mathbf{w}^*} \leq \eta \sup_{\|D\|_{\mathbf{w}^*} \leq r_1} \|\mathbf{h}(\tilde{\mathbf{w}}(D))\|_{\mathbf{w}^*} < r_1,$$

the last one is again due to the assumption (31) on η . The smoothness of F then follows.

Regarding the estimate over $\|F(D)\|_{\mathbf{w}^*}$, we first expand F around origin up to the first order: there exist constants $r_3 \in (0, r_2]$ and $c_3 \geq 0$ such that

$$F(D) = F(D) - F(0) = DF(0)[D] + r(D), \quad \forall D \in \mathrm{T}_{\mathbf{w}^*}(\mathrm{Gr}_k(\mathrm{T}\mathcal{M})) : \|D\|_{\mathbf{w}^*} < r_3,$$

where $r(D) := (r_1(D), r_2(D))$ collects the higher-order terms and satisfies

$$\|r_1(D)\|, \|r_2(D)_{\mathbf{x}^*}\| < c_3 (\|\delta\|^2 + \|\Delta_{\mathbf{x}^*}\|^2),$$

with $r_2(D)_{\mathbf{x}^*}$ defined in a similar way as in Eq. (19). More calculations on the first-order term yield that

$$\begin{aligned} DF(0)[D] &= \mathrm{D}\mathrm{Retr}^{\mathrm{Gr}_k(\mathrm{T}\mathcal{M})}(\mathbf{w}^*, 0) [(D, \eta \cdot \mathrm{D}\mathbf{h}(\mathbf{w}^*)[D])] = D + \eta \cdot \mathrm{D}\mathbf{h}(\mathbf{w}^*)[D] \\ &= \begin{pmatrix} \delta - \eta R_{\mathbf{w}^*}(\mathrm{Hess}_{\mathcal{M}} f(\mathbf{x}^*)[\delta]) \\ \Delta - \eta [P^*, [\Delta, \mathrm{Hess}_{\mathcal{M}} f(\mathbf{x}^*)]] + \eta \mathbf{m}_3(\mathbf{w}^*)[\delta] \end{pmatrix}, \end{aligned}$$

where the second equality follows from [13, Lemma 4.21] and the last one uses Eq. (29). In all, we have

$$\begin{aligned} \|F_1(D)\| &= \|\delta - \eta R_{\mathbf{w}^*}(\mathrm{Hess}_{\mathcal{M}} f(\mathbf{x}^*)[\delta]) + r_1(D)\| \\ &\leq \|\mathrm{Id}_{\mathbf{T}_{\mathbf{x}^*}\mathcal{M}} - \eta R_{\mathbf{w}^*} \circ \mathrm{Hess}_{\mathcal{M}} f(\mathbf{x}^*)\| \|\delta\| + c_3 (\|\delta\|^2 + \|\Delta_{\mathbf{x}^*}\|^2) \\ &\leq (q_1(\eta) + c_3 r_3) \|\delta\| + c_3 r_3 \|\Delta_{\mathbf{x}^*}\|, \end{aligned}$$

and

$$\begin{aligned}
\|F_2(D)_{\mathbf{x}^*}\| &= \|\text{Proj}_{T_{\mathbf{x}^*}\mathcal{M}} \circ F_2(D) \circ \text{Proj}_{T_{\mathbf{x}^*}\mathcal{M}}\| \\
&= \|\Delta_{\mathbf{x}^*} - \eta[P^*, [\Delta_{\mathbf{x}^*}, \text{Hess}_{\mathcal{M}} f(\mathbf{x}^*)]] + (\mathbf{m}_3(\mathbf{w}^*)[\delta])_{\mathbf{x}^*} + r_2(D)_{\mathbf{x}^*}\| \\
&\leq \|\text{Id}_{T_{P^*}\text{Gr}_k(T_{\mathbf{x}^*}\mathcal{M})} - \eta[P^*, [\text{Id}_{T_{P^*}\text{Gr}_k(T_{\mathbf{x}^*}\mathcal{M})}, \text{Hess}_{\mathcal{M}} f(\mathbf{x}^*)]]\| \|\Delta_{\mathbf{x}^*}\| \\
&\quad + \eta \|\mathbf{m}_3(\mathbf{w}^*)_{\mathbf{x}^*}\| \|\delta\| + c_3 r_3 (\|\delta\| + \|\Delta_{\mathbf{x}^*}\|) \\
&\leq (q_2(\eta) + c_3 r_3) \|\Delta_{\mathbf{x}^*}\| + (\eta M + c_3 r_3) \|\delta\|.
\end{aligned}$$

The proof is complete. \square

Lemma 8. *Let X be a 2×2 matrix with distinct eigenvalues μ_1 and μ_2 . Then for any $t \in \mathbb{N}$, it holds that*

$$X^t = \frac{\mu_1^t - \mu_2^t}{\mu_1 - \mu_2} X - \frac{\mu_2 \mu_1^t - \mu_1 \mu_2^t}{\mu_1 - \mu_2} I_2.$$

Proof. Since X is 2×2 , the Cayley-Hamilton theorem tells us that X satisfies its own characteristic equation:

$$X^2 - (\mu_1 + \mu_2)X + \mu_1 \mu_2 I_2 = 0. \quad (33)$$

In what follows, we prove the desired result by induction. The conclusion holds obviously for the cases of $t = 0, 1, 2$. Now suppose that the conclusion holds for the case of $t = \ell \in \mathbb{N}$ and consider the case of $t = \ell + 1$. Direct calculations yield

$$\begin{aligned}
X^{\ell+1} &= X^\ell \cdot X = \left(\frac{\mu_1^\ell - \mu_2^\ell}{\mu_1 - \mu_2} X - \frac{\mu_2 \mu_1^\ell - \mu_1 \mu_2^\ell}{\mu_1 - \mu_2} I_2 \right) X \\
&= \frac{\mu_1^\ell - \mu_2^\ell}{\mu_1 - \mu_2} ((\mu_1 + \mu_2)X - \mu_1 \mu_2 I_2) - \frac{\mu_2 \mu_1^\ell - \mu_1 \mu_2^\ell}{\mu_1 - \mu_2} X \\
&= \frac{\mu_1^{\ell+1} - \mu_2^{\ell+1}}{\mu_1 - \mu_2} X - \frac{\mu_2 \mu_1^{\ell+1} - \mu_1 \mu_2^{\ell+1}}{\mu_1 - \mu_2} I_2.
\end{aligned}$$

Here the second equality follows from mathematical induction and the third one uses Eq. (33). As a result, the conclusion holds for the case of $t = \ell + 1$ as well. The proof is complete. \square

Theorem 3 (Local convergence of Algorithm 1). *Suppose that f is C^3 , \mathcal{M} is a Riemannian submanifold of a Euclidean space \mathcal{E} with $\dim(\mathcal{M}) = d$, $\mathbf{x}^* \in \mathcal{M}$ is an index- k constrained SP of f over \mathcal{M} , $\text{Hess}_{\mathcal{M}} f(\mathbf{x}^*)$ is nondegenerate, whose eigenvalues are $\lambda_1^* \leq \dots \leq \lambda_k^* < 0 < \lambda_{k+1}^* \leq \dots \leq \lambda_d^*$, and $P^* \in \text{Gr}_k(T_{\mathbf{x}^*}\mathcal{M})$ is an orthogonal projector onto the lowest k -dimensional invariant subspace of $\text{Hess}_{\mathcal{M}} f(\mathbf{x}^*)$. Let $\mathbf{w}^* := (\mathbf{x}^*, P^*) \in \text{Gr}_k(T\mathcal{M})$ and $\{\mathbf{w}^{(t)} := (\mathbf{x}^{(t)}, P^{(t)})\}$ be the sequence generated by Algorithm 1. If the following two assumptions hold:*

- (Smallness of the step size) *the step size fulfills*

$$0 < \eta < \min \left\{ \frac{2}{\Delta \lambda_{d1}^*}, \frac{q_1(\eta) + q_2(\eta)}{M}, \frac{\min\{(r_1 - r_2)/c_1, r_1\}}{\sup_{\|D\|_{\mathbf{w}^*} \leq r_1} \|\mathbf{h}(\mathbf{w}(D))\|_{\mathbf{w}^*}} \right\} \quad (34)$$

with c_1 and r_1 the constants in Lemma 6 (associated to $\mathcal{N} = \text{Gr}_k(T\mathcal{M})$, $\text{Retr}^{\mathcal{N}} = \text{Retr}^{\text{Gr}_k(T\mathcal{M})}$ or $\text{Exp}^{\text{Gr}_k(T\mathcal{M})}$, and $\mathbf{y} = \mathbf{w}^$) and $r_2 \in (0, r_1)$;*

- (Proximity of the initial point to the desired constrained SP) *the initial point satisfies*

$$\text{dist}_{\text{Gr}_k(T\mathcal{M})}(\mathbf{w}^*, \mathbf{w}^{(0)}) < \frac{r_3}{\max \left\{ \max \left\{ \frac{\mu_1(\eta)^2}{\mu_1(\eta) - \mu_2(\eta)}, 1 \right\} \|A(\eta)\|, 1 \right\}}, \quad (35)$$

where the constants c_3 and r_3 are defined in Lemma 7 and are chosen such that

$$c_3 r_3 < \frac{(1 - q_{\max}(\eta))^2}{\eta M + 2(1 - q_{\max}(\eta))} \quad \text{with} \quad q_{\max}(\eta) := \max \{q_1(\eta), q_2(\eta)\}, \quad (36)$$

and $\mu_1(\eta)$, $\mu_2(\eta)$ are respectively

$$\begin{aligned}\mu_1(\eta) &:= \frac{q_1(\eta) + q_2(\eta) + 2c_3r_3 + \sqrt{(q_1(\eta) - q_2(\eta))^2 + 4c_3r_3(\eta M + c_3r_3)}}{2}, \\ \mu_2(\eta) &:= \frac{q_1(\eta) + q_2(\eta) + 2c_3r_3 - \sqrt{(q_1(\eta) - q_2(\eta))^2 + 4c_3r_3(\eta M + c_3r_3)}}{2},\end{aligned}\tag{37}$$

then $\{\mathbf{w}^{(t)}\}$ converges linearly to \mathbf{w}^* .

Proof. We first show by induction that $\text{dist}_{\text{Gr}_k(\text{T}\mathcal{M})}(\mathbf{w}^*, \mathbf{w}^{(t)}) < r_3$ holds for any t , so that $\text{Exp}_{\mathbf{w}^*}^{\text{Gr}_k(\text{T}\mathcal{M})}$ remains a diffeomorphism and Eq. (32) is applicable for all the iterates. The case of $t = 0$ is evident due to the assumption (35) on the initial point. Now suppose that the statement holds for the case of $t = \ell \in \mathbb{N}$ and consider the case of $t = \ell + 1$. By induction and Eq. (32), there exists a unique $D^{(\ell+1)} \in \text{T}_{\mathbf{w}^*}(\text{Gr}_k(\text{T}\mathcal{M}))$ such that $\|D^{(\ell+1)}\|_{\mathbf{w}^*} < r_3$ and $D^{(\ell+1)} = F(D^{(\ell)})$ hold for $t = 0, \dots, \ell - 1$, and that

$$\begin{pmatrix} \|F_1(D^{(\ell)})\| \\ \|F_2(D^{(\ell)})_{\mathbf{x}^*}\| \end{pmatrix} \leq A(\eta)^{\ell+1} \begin{pmatrix} \|\delta^{(0)}\| \\ \|\Delta_{\mathbf{x}^*}^{(0)}\| \end{pmatrix}.\tag{38}$$

It is not difficult to verify that $\mu_1(\eta)$ and $\mu_2(\eta)$ in Eq. (37) are the two distinct real eigenvalues of $A(\eta)$, and both of them belong to $(0, 1)$:

$$\begin{aligned}2\mu_2(\eta) &= q_1(\eta) + q_2(\eta) + 2c_3r_3 - \sqrt{(q_1(\eta) - q_2(\eta))^2 + 4c_3r_3(\eta M + c_3r_3)} \\ &> q_1(\eta) + q_2(\eta) + 2c_3r_3 - \sqrt{(q_1(\eta) - q_2(\eta))^2 + 4c_3r_3(q_1(\eta) + q_2(\eta) + c_3r_3)} \\ &= q_1(\eta) + q_2(\eta) + 2c_3r_3 - \sqrt{(q_1(\eta) + q_2(\eta) + 2c_3r_3)^2 - 4q_1(\eta)q_2(\eta)} \geq 0,\end{aligned}$$

where the strict inequality is due to the assumption (34), and

$$\begin{aligned}2\mu_1(\eta) &= q_1(\eta) + q_2(\eta) + 2c_3r_3 + \sqrt{(q_1(\eta) - q_2(\eta))^2 + 4c_3r_3(\eta M + c_3r_3)} \\ &\leq q_1(\eta) + q_2(\eta) + 2c_3r_3 + |q_1(\eta) - q_2(\eta)| + 2\sqrt{c_3r_3(\eta M + c_3r_3)} \\ &= 2 \left(c_3r_3 + q_{\max}(\eta) + \sqrt{c_3r_3(\eta M + c_3r_3)} \right) \\ &< 2 \left(\frac{(1 - q_{\max}(\eta))^2}{\eta M + 2(1 - q_{\max}(\eta))} + q_{\max}(\eta) + \sqrt{\frac{(1 - q_{\max}(\eta))^2(\eta M + 1 - q_{\max}(\eta))^2}{(\eta M + 2(1 - q_{\max}(\eta)))^2}} \right) \\ &= 2 \left(\frac{(1 - q_{\max}(\eta))^2}{\eta M + 2(1 - q_{\max}(\eta))} + q_{\max}(\eta) + \frac{(1 - q_{\max}(\eta))(\eta M + 1 - q_{\max}(\eta))}{\eta M + 2(1 - q_{\max}(\eta))} \right) = 2,\end{aligned}$$

where the strict inequality uses the assumption (36) and the third equality uses $q_1(\eta), q_2(\eta) < 1$ from the assumption (34). By Lemma 8,

$$\begin{aligned}A(\eta)^{\ell+1} \begin{pmatrix} \|\delta^{(0)}\| \\ \|\Delta_{\mathbf{x}^*}^{(0)}\| \end{pmatrix} &= \left(\frac{\mu_1(\eta)^{\ell+1} - \mu_2(\eta)^{\ell+1}}{\mu_1(\eta) - \mu_2(\eta)} A(\eta) - \frac{\mu_2(\eta)\mu_1(\eta)^{\ell+1} - \mu_1(\eta)\mu_2(\eta)^{\ell+1}}{\mu_1(\eta) - \mu_2(\eta)} I_2 \right) \begin{pmatrix} \|\delta^{(0)}\| \\ \|\Delta_{\mathbf{x}^*}^{(0)}\| \end{pmatrix} \\ &\leq \max \left\{ \frac{\mu_1(\eta)^2}{\mu_1(\eta) - \mu_2(\eta)}, 1 \right\} A(\eta) \begin{pmatrix} \|\delta^{(0)}\| \\ \|\Delta_{\mathbf{x}^*}^{(0)}\| \end{pmatrix},\end{aligned}\tag{39}$$

where the inequality is due to $0 < \mu_2(\eta) < \mu_1(\eta) < 1$. Eqs. (38), (39), and the assumption (35) on the initial point then together imply

$$\|F(D^{(\ell)})\|_{\mathbf{w}^*}^2 = \|F_1(D^{(\ell)})\|^2 + \|F_2(D^{(\ell)})_{\mathbf{x}^*}\|^2 = \left\| A(\eta)^{\ell+1} \begin{pmatrix} \|\delta^{(0)}\| \\ \|\Delta_{\mathbf{x}^*}^{(0)}\| \end{pmatrix} \right\|^2$$

$$\begin{aligned}
&\leq \max \left\{ \frac{\mu_1(\eta)^2}{\mu_1(\eta) - \mu_2(\eta)}, 1 \right\}^2 \left\| A(\eta) \begin{pmatrix} \|\delta^{(0)}\| \\ \|\Delta_{\mathbf{x}^*}^{(0)}\| \end{pmatrix} \right\|^2 \\
&\leq \max \left\{ \frac{\mu_1(\eta)^2}{\mu_1(\eta) - \mu_2(\eta)}, 1 \right\}^2 \|A(\eta)\|^2 \|D^{(0)}\|_{\mathbf{w}^*}^2 < r_3^2.
\end{aligned}$$

Consequently, there exists a unique $D^{(\ell+1)} \in \mathbf{T}_{\mathbf{w}^*}(\mathrm{Gr}_k(\mathrm{T}\mathcal{M}))$ such that $\|D^{(\ell+1)}\| < r_3$ and $D^{(\ell+1)} = F(D^{(\ell)})$. The statement thus holds for any $k \in \mathbb{N}$.

Now by Eqs. (38) and (39), we have for any $k \geq 1$ that

$$\begin{pmatrix} \|\delta^{(t)}\| \\ \|\Delta_{\mathbf{x}^*}^{(t)}\| \end{pmatrix} \leq \left(\frac{\mu_1(\eta)^t - \mu_2(\eta)^t}{\mu_1(\eta) - \mu_2(\eta)} A(\eta) - \frac{\mu_2(\eta)\mu_1(\eta)^t - \mu_1(\eta)\mu_2(\eta)^t}{\mu_1(\eta) - \mu_2(\eta)} I_2 \right) \begin{pmatrix} \|\delta^{(0)}\| \\ \|\Delta_{\mathbf{x}^*}^{(0)}\| \end{pmatrix},$$

which combined with $0 \leq \mu_2(\eta) < \mu_1(\eta) < 1$ and $\|D^{(t)}\|_{\mathbf{w}^*}^2 = \|\delta^{(t)}\|^2 + \|\Delta_{\mathbf{x}^*}^{(t)}\|^2$ implies that $D^{(t)}$ converges linearly to 0, or equivalently, $\{\mathbf{w}^{(t)}\}$ converges linearly to \mathbf{w}^* as $k \rightarrow \infty$. The proof is completed. \square

Remark 2 (Satisfiability of the assumptions). *It might seem to be difficult at first glance to check the satisfiability of the assumptions (34) and (36). Indeed, after noting that $q_1(\eta)$, $q_2(\eta) \rightarrow 1-$ as $\eta \rightarrow 0+$, the assumption (34) can always be met with a sufficiently small η . Once η is fixed, one could choose an r_3 small enough to meet the assumption (36), since c_3 , as a function of r_3 , is uniformly bounded in a small neighborhood of origin.*

Remark 3 (Local convergence rates and condition numbers). *Lemma 7 provides some information about the local convergence rates of \mathbf{x} - and P -residuals. Indeed, as long as r_3 is sufficiently small, the contraction matrix $A(\eta)$ in Eq. (32) becomes close to diagonal, with entries dominated by $q_1(\eta)$ and $q_2(\eta)$. They can then be viewed as the contractive factors of \mathbf{x} - and P -residuals, respectively.*

Moreover, if two different step sizes $\eta_{\mathbf{x}}$ and η_P are used, it is possible for us to approach the best linear convergence rates. By the definitions of $q_1(\eta)$ and $q_2(\eta)$ in Lemma 7, it is easy to show that the step sizes minimizing these two terms are

$$\eta_{\mathbf{x}}^* := \frac{2}{\lambda_{\min}^* + \lambda_{\max}^*} = \frac{2}{\min_{i=1}^d |\lambda_i^*| + \max_{i=1}^d |\lambda_i^*|}, \quad (40)$$

$$\eta_P^* := \frac{2}{\Delta\lambda_{k+1,k}^* + \Delta\lambda_{d1}^*} = \frac{2}{\lambda_d^* + \lambda_{k+1}^* - \lambda_k^* - \lambda_1^*}. \quad (41)$$

The condition numbers are thus estimated by

$$\kappa_{\mathbf{x}} := \frac{\lambda_{\max}^*}{\lambda_{\min}^*} = \frac{\max_{i=1}^d |\lambda_i^*|}{\min_{i=1}^d |\lambda_i^*|}, \quad \kappa_P := \frac{\Delta\lambda_{d1}^*}{\Delta\lambda_{k+1,k}^*} = \frac{\lambda_d^* - \lambda_1^*}{\lambda_{k+1}^* - \lambda_k^*}. \quad (42)$$

We shall note that the best step sizes in practice are not necessarily given by Eqs. (40) and (41) exactly, since Eq. (32) provides only an estimate from above and the terms other than $q_1(\eta)$ and $q_2(\eta)$ in the contraction matrix $A(\eta)$ might not be negligible. For numerical illustrations, see Section 5.1.

Remark 4 (Comparison with the existing results for discretized algorithms). *All the existing results [30, 33, 50, 58, 59, 91] are set in the unconstrained settings. Therefore, it makes no sense to conduct a direct comparison. Nevertheless, we shall point out that the local convergence rate and condition number for the \mathbf{x} -residual in Remark 3 recover the ones in [59] if we let $\mathcal{M} = \mathcal{E}$, yet with weaker assumptions on the eigenvalues of the Hessian (see Remark 1). Moreover, since we treat \mathbf{x} and P equally over the Grassmann bundle $\mathrm{Gr}_k(\mathrm{T}\mathcal{M})$, by leveraging the geometrical tools, we manage to establish the explicit local convergence rates and condition*

numbers for both parts in the manifold constrained settings (see Remark 3), and do not require unnecessary (or even uncheckable) assumptions; for example, the angle assumption in [59], which reads

$$\exists \alpha \in [0, 1), \text{ s. t. } \left\| V^{(t)}(V^{(t)})^\top - V(\mathbf{x}^{(t)})V(\mathbf{x}^{(t)})^\top \right\| \leq \alpha, \forall t.$$

Here, $V(\mathbf{x}^{(t)}) \in \text{St}_k(\text{T}_{\mathbf{x}^{(t)}}\mathcal{M})$ spans exactly the lowest k -dimensional invariant subspace of $\text{Hess}_{\mathcal{M}} f(\mathbf{x}^{(t)})$.

Example 2 (Condition numbers at index-1 constrained SPs). Consider a linear objective function over $\mathcal{M} = \text{Gr}_p(\mathbb{R}^n)$ ($p > 1$) defined by $f(P) = \text{Tr}(PA)$ for any $P \in \mathcal{M}$, where $A \in \mathbb{R}_{\text{sym}}^{n \times n}$. It is not difficult to obtain the closed-form expression of Riemannian Hessian:

$$\text{Hess}_{\mathcal{M}} f(P)[\Gamma] = [P, [\Gamma, A]], \quad \forall P \in \mathcal{M}, \Gamma \in \text{T}_P\mathcal{M}.$$

For simplicity, suppose that A is diagonal, i.e., $A = \text{diag}(\varepsilon_1, \dots, \varepsilon_n)$ with $\varepsilon_1 \leq \dots \leq \varepsilon_n$, and that all the sums of p eigenvalues of A are different. Under this assumption, one could verify that the unique global minimizer (GM) and unique index-1 constrained SP of f over \mathcal{M} are respectively

$$P_{\text{GM}} := \sum_{i=1}^p \mathbf{e}_i \mathbf{e}_i^\top \quad \text{and} \quad P_{\text{SP}} := \sum_{i=1}^{p-1} \mathbf{e}_i \mathbf{e}_i^\top + \mathbf{e}_{p+1} \mathbf{e}_{p+1}^\top,$$

where \mathbf{e}_i is the i -th unit vector in \mathbb{R}^n ($i = 1, \dots, n$). The eigenpairs of $\text{Hess}_{\mathcal{M}} f(P_{\text{GM}})$ are given explicitly by

$$\left\{ \left(\varepsilon_a - \varepsilon_i, \frac{1}{\sqrt{2}} (\mathbf{e}_i \mathbf{e}_a^\top + \mathbf{e}_a \mathbf{e}_i^\top) \right) \middle| i = 1, \dots, p, a = p+1, \dots, n \right\},$$

and for $\text{Hess}_{\mathcal{M}} f(P_{\text{SP}})$,

$$\left\{ \left(\varepsilon_a - \varepsilon_i, \frac{1}{\sqrt{2}} (\mathbf{e}_i \mathbf{e}_a^\top + \mathbf{e}_a \mathbf{e}_i^\top) \right) \middle| i = 1, \dots, p-1, p+1, a = p, p+2, \dots, n \right\}.$$

The condition number at P_{GM} is

$$\kappa_{P_{\text{GM}}} = \frac{\varepsilon_n - \varepsilon_1}{\varepsilon_{p+1} - \varepsilon_p},$$

which is well known in the literature. The denominator is also called the “eigengap” in some applications. Regarding the condition number at P_{SP} , with reference to Eq. (42), we could identify $\lambda_1^* = \varepsilon_p - \varepsilon_{p+1} < 0$, $\lambda_2^* = \min\{\varepsilon_{p+2} - \varepsilon_{p+1}, \varepsilon_p - \varepsilon_{p-1}\} > 0$, and $\lambda_d^* = \varepsilon_n - \varepsilon_1 > 0$ (with $d = \dim(\mathcal{M}) = p(n-p)$), and therefore,

$$\lambda_{\min}^* = \min \{\varepsilon_p - \varepsilon_{p-1}, \varepsilon_{p+1} - \varepsilon_p, \varepsilon_{p+2} - \varepsilon_{p+1}\}, \quad \lambda_{\max}^* = \varepsilon_n - \varepsilon_1,$$

which implies

$$\kappa_{P_{\text{SP}}} = \frac{\varepsilon_n - \varepsilon_1}{\min \{\varepsilon_p - \varepsilon_{p-1}, \varepsilon_{p+1} - \varepsilon_p, \varepsilon_{p+2} - \varepsilon_{p+1}\}}.$$

Comparing $\kappa_{P_{\text{SP}}}$ with $\kappa_{P_{\text{GM}}}$, we observe that finding the index-1 constrained SPs can be worse conditioned. Moreover, it asks for not only a positive eigengap, but also nondegeneracy above ε_{p+1} and below ε_p . Another useful message is that, if the problem is reformulated on the Stiefel manifold $\text{St}_p(\mathbb{R}^n)$ and is treated by the saddle search algorithms in the existing works [52, 54, 87, 90], we could anticipate their poor performance due to the inherent degeneracy. For illustrations, see Section 5.1.

5 Numerical experiments

In this part, we report numerical results on the linear eigenvalue problem and electronic excited-state calculations. Both tasks sit on the Grassmann manifold. In particular, with the former one, we elucidate the importance of using nonredundant parametrizations in finding SPs (cf. Example 2) and show the influence of problem and algorithm settings on the convergence rates (cf. Remark 3).

5.1 Linear eigenvalue problem

Given a real symmetric matrix $A \in \mathbb{R}_{\text{sym}}^{n \times n}$, the linear eigenvalue problem amounts to finding a critical point X^* of the quadratic function $f_{\text{St}}(X) := \frac{1}{2}\text{Tr}(X^\top AX)$ over the Stiefel manifold $\text{St}_p(\mathbb{R}^n)$. It is well known that the columns of any such point span a p -dimensional invariant subspace of A . Moreover, the function value $f_{\text{St}}(X^*)$ is exactly half the sum of p eigenvalues of A . If all the sums ($\binom{n}{p}$ in total) are different from each other, the indices of the saddle points can be indicated by their function values, in that $f_{\text{St}}(X_{\text{SP},k}^*) < f_{\text{St}}(X_{\text{SP},\ell}^*)$ holds for the index- k and index- ℓ constrained SPs whenever $k < \ell$ (the reverse might not be true). Note that f_{St} is invariant under the transformation $X \mapsto XQ$ for any $Q \in \mathcal{O}(p)$. Therefore, one could instead consider a linear function $f_{\text{Gr}}(P) := \frac{1}{2}\text{Tr}(PA)$ over the Grassmann manifold $\text{Gr}_p(\mathbb{R}^n)$ and any of its critical point P^* is the orthogonal projector onto a p -dimensional invariant subspace of A . The statements regarding the function values and indices of constrained SPs remain valid similarly.

Implementation details. In what follows, we construct the test matrix A as $A = U\Sigma U^\top$, where $U \in \mathcal{O}(n)$ is obtained from the orthonormalization of a matrix whose entries are random numbers drawn independently and identically from the standard normal distribution (random seed = 0), and $\Sigma = \text{diag}(\sigma_1, \dots, \sigma_n) \in \mathbb{R}^{n \times n}$ with $\sigma_i := \xi^{i-n}$ ($i = 1, \dots, n$) for a parameter $\xi > 1$. The problem data n , p , and ξ are specified later. We consider Algorithm 2 of Stiefel and Grassmann versions ($\mathcal{M} = \text{St}_p(\mathbb{R}^n)$ and $\mathcal{M} = \text{Gr}_p(\mathbb{R}^n)$). For simplicity, we do not implement the retractions in Eqs. (20) and (21); for the position part, we adopt the QR decomposition-based second-order retraction over $\text{St}_p(\mathbb{R}^n)$ and the exponential mapping over $\text{Gr}_p(\mathbb{R}^n)$, respectively, whereas for the direction part, we perform orthogonal projections onto the new tangent space. The step sizes are specified later. The maximum iteration number and convergence tolerance are respectively set as $\text{maxit} = \infty$ and $\text{tol} = 10^{-8}$. If not stated, the initial feasible points $(X^{(0)}, V^{(0)})$ and $(P^{(0)}, \Gamma^{(0)})$ are randomly generated as follows: with a given random seed,

```

from jax import random, numpy
key = random.PRNGKey(randseed) # random seed
key1, key2 = random.split(key)
X, _ = numpy.linalg.qr(random.normal(key1, (n, p)))
P = X @ X.T
Gamma = random.normal(key2, (n, n))
Gamma = (Gamma + Gamma.T) / 2.0
Gamma = proj_tangent(P, Gamma) # project onto the tangent space
V = Gamma @ X # horizontal lift

```

Importance of nonredundant parametrizations. Let $n = 64$, $p = 8$, and $\xi = 1.01$. Following the above problem description, we run both the Stiefel and Grassmann versions of Algorithm 2 to find the index-1 constrained SPs of f_{St} and f_{Gr} , respectively. The initial feasible points are generated with random seed = 1. The step sizes are specified as $\eta_{\text{St}} = 2$ and $\eta_{\text{Gr}} = 4$. The convergence curves are depicted in Figure 1.

We first observe from the left panel of Figure 1 the convergence of both versions of the

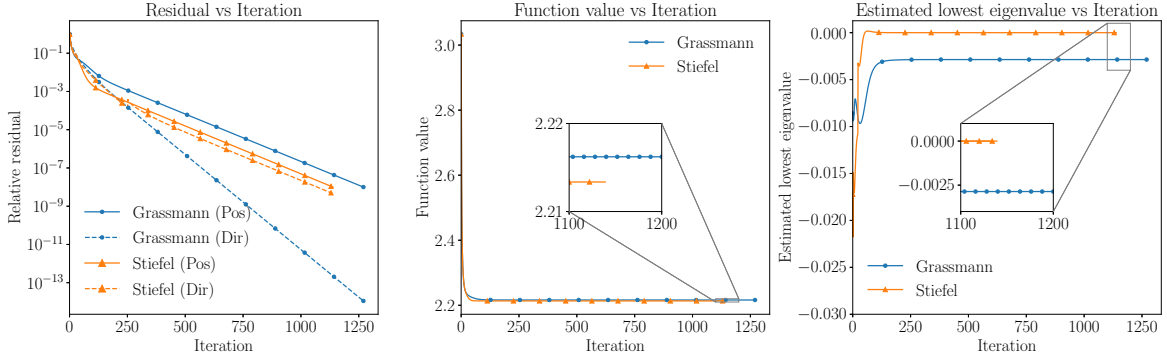


Figure 1: Convergence curves of Algorithm 2 of Stiefel (orange lines) and Grassmann (blue lines) versions on the linear eigenvalue problem ($n = 64$, $p = 8$, and $\xi = 1.01$). Left: position (solid lines) and direction (dashed lines) relative residuals vs iteration. Middle: function value vs iteration. Right: estimated lowest eigenvalue of Riemannian Hessian vs iteration.

algorithm. The correctness of the results can be checked by comparing the function values; see the middle panel of Figure 1. Due to the construction of A , the function value at the index-1 constrained SP is exactly $\frac{1}{2}(\sum_{i=1}^{p-1} \sigma_i + \sigma_{p+1}) \approx 2.216$. Initialized from the same point (more precisely, the Stiefel version is fed with the representative of the initial point for the Grassmann version), the Grassmann version converges well to the desired constrained SP, while the Stiefel one gets trapped to the global minimizer, whose function value is $\frac{1}{2} \sum_{i=1}^p \sigma_i \approx 2.213$. This comparison can also be seen in the right panel of Figure 1, where the Riemannian Hessian at the point given by the Stiefel version is found to be positive semidefinite.

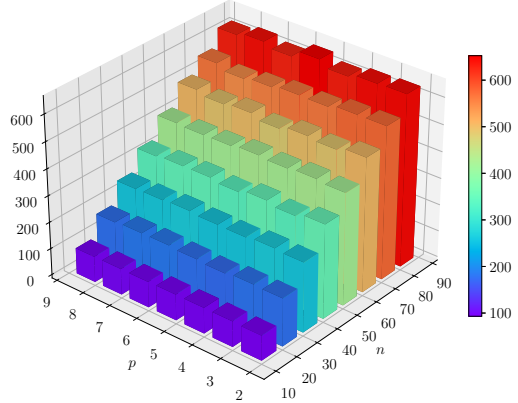
We remark that the failure of the Stiefel version should be ascribed to the parametrization redundancy. The formulation over the Stiefel manifold does not take into account the quotient structure, as explained in the first paragraph of this subsection. The redundancy brings degeneracies above and/or below the eigengap and leads to an infinite condition number at the desired index-1 constrained SP (cf. Example 2). The deficiency cannot be neglected as in the task of finding the global minimizer because the update direction for the position is not a horizontal lift of that in the Grassmann version. Roughly, suppose that the initial point lies in a region where the Riemannian Hessian is positive semidefinite (say, around the global minimizer) and the direction step converges quickly to the lowest eigenvector of the Riemannian Hessian. Due to the parametrization redundancy, the lowest eigenvalue of the Riemannian Hessian is zero and the direction variable $V(t)$ is almost vertical. This implies that climbing up along $V(t)$ makes little difference in the first order and the position variable mainly follows the gradient flow down to the minimizer.

The above arguments are supported with numerical results. We run the Grassmann and Stiefel algorithms with the same problem and algorithm settings as before and randomly sampled initial points perturbed from the global minimizer and index-1 constrained SP. Specifically, we consider the perturbation level $\beta \in \{10^{-3}, 10^{-2}, \dots, 10^1\}$ and each of them is tested

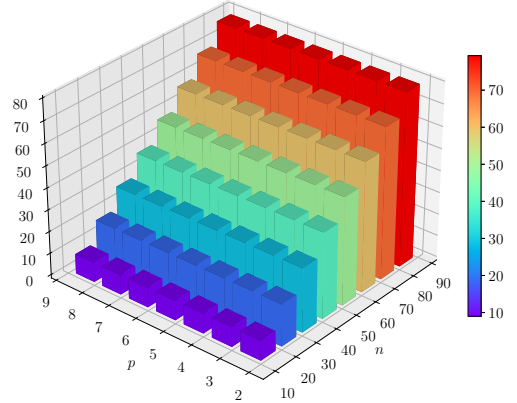
Table 1: Empirical success rates in finding the index-1 constrained SP of Algorithm 2 of Grassmann and Stiefel versions starting from the neighborhoods of the global minimizer and index-1 constrained SP of the linear eigenvalue problem ($n = 64$, $p = 8$, and $\xi = 1.01$).

Algorithms	Perturbation from global minimizer					Perturbation from constrained SP				
	10^{-3}	10^{-2}	10^{-1}	10^0	10^1	10^{-3}	10^{-2}	10^{-1}	10^0	10^1
Grassmann	100%	100%	100%	100%	100%	100%	100%	100%	100%	100%
Stiefel	0%	0%	0%	29%	33%	100%	98%	59%	25%	30%

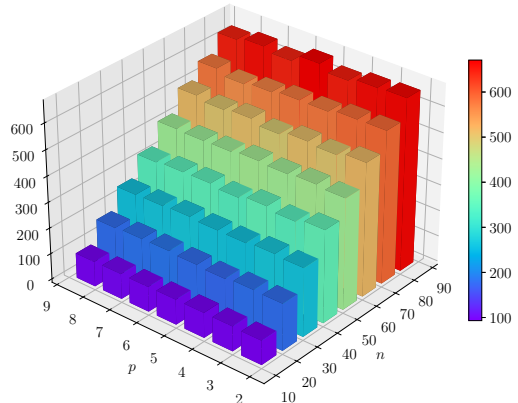
Averaged iteration number



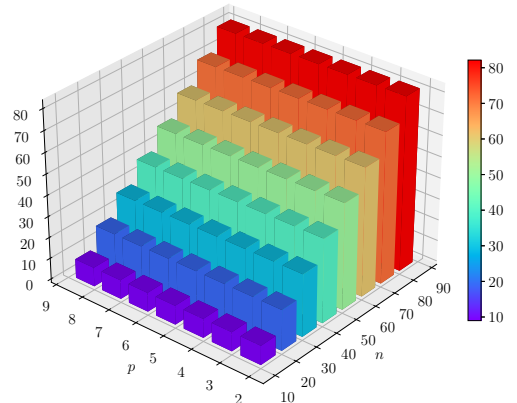
Condition number

(a) $\xi = 1.0001$.

Averaged iteration number



Condition number

(b) $\xi = 1.001$.Figure 2: Average iteration number (left) and estimated condition number (right) vs (n, p) on the linear eigenvalue problem class.

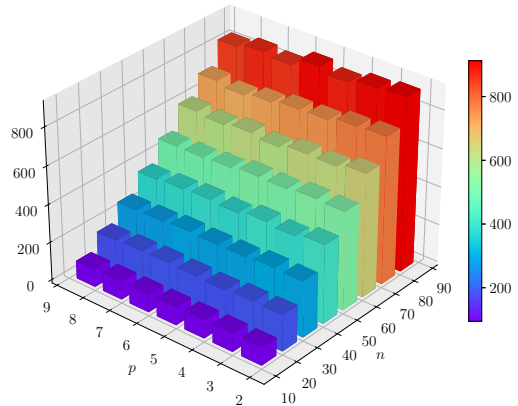
with 100 independent random samples (random seed = $0 \sim 99$):

```
key = random.PRNGKey(randseed) # random seed
key1, key2 = random.split(key)
X, _ = numpy.linalg.qr(X_ref + beta * random.normal(key1, (n, p)))
# repeat previous procedures to create P, Gamma, and V
```

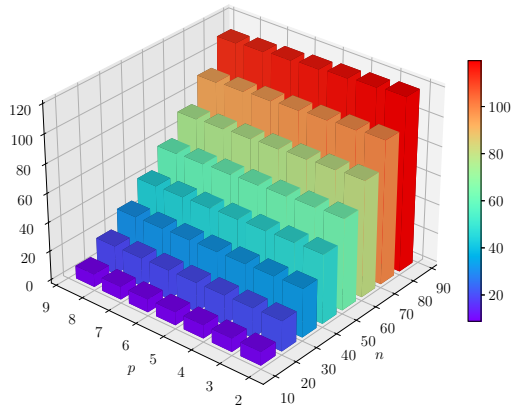
Here X_{ref} is either the global minimizer or index-1 constrained SP. The empirical success rates of the two algorithms at different perturbation levels are recorded in Table 1. It turns out that the Grassmann version converges surprisingly well across the board to the index-1 constrained SP, whereas the Stiefel one often gets attracted by the global minimizer, with an empirical success rate of approximately 30% if randomly initialized. The rate can be tremendously improved if the initial point is selected around the desired index-1 constrained SP. We only use the Grassmann version for the subsequent experiments.

Influence of problem and algorithm settings on the convergence rates. We investigate the performance of Algorithm 2 in finding the index-1 constrained SP with different problem data (n , p , and ξ) and algorithm settings (initialization and step sizes). First consider varying the problem data in $n \in \{10, 20, \dots, 80\}$, $p \in \{2, 3, \dots, 8\}$, $\xi \in \{1.0001, 1.001, 1.01, 1.05\}$. The step sizes are determined by the estimates (40) and (41).

Averaged iteration number



Condition number

(a) $\xi = 1.01$.

Averaged iteration number

Condition number

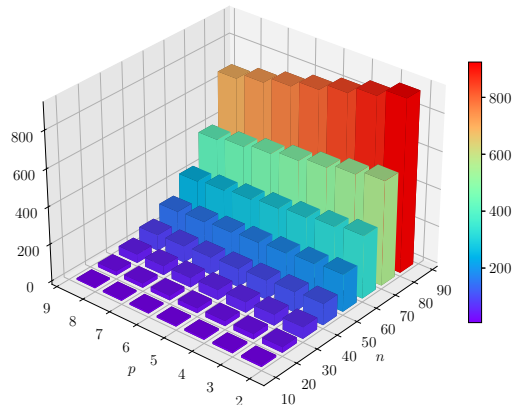
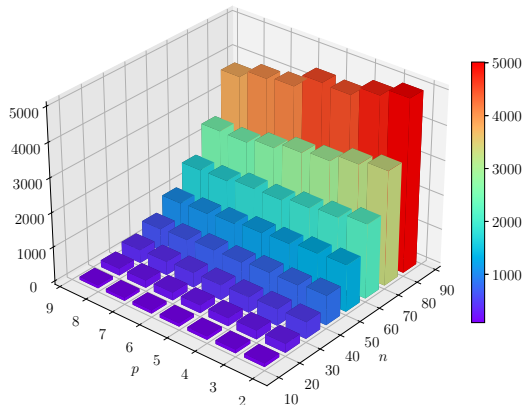
(b) $\xi = 1.05$.

Figure 3: Average iteration number (left) and estimated condition number (right) vs (n, p) on the linear eigenvalue problem class.

For each problem setting, we perform ten independent runs of the algorithm with the initial points randomly selected at the perturbation level of 10^{-3} from the index-1 constrained SP (random seed = 0 ~ 9). The average iteration numbers and the condition numbers estimated through Eq. (42), $\kappa = \frac{\xi^{n-1}-1}{\xi^{p-2}(\xi-1)}$, are shown with bar plots in Figures 2 and 3. The trends of the iteration numbers are found to align qualitatively well with those of the estimated condition numbers, showcasing the validity of our theoretical analysis.

Next we consider varying the algorithm settings. We fix the problem data to be $n = 10$, $p = 2$, and $\xi = 1.01$. Since the best step sizes are estimated by Eqs. (40) and (41) to be $(\eta_P^*, \eta_\Gamma^*) \approx (21.096, 17.656)$ for this instance, the step sizes η_P and η_Γ are varied in $\{10, 12, \dots, 30\}$. For each pair of (η_P, η_Γ) , we perform ten independent runs of the algorithm with the initial points randomly selected at the perturbation level of 10^{-3} or 10^{-1} from the index-1 constrained SP (random seed = 0 ~ 9). Similarly, we visualize the results with bar plots in Figure 4. For this test instance, the least iteration numbers are achieved when the pair $(\eta_P, \eta_\Gamma) = (30, 30)$ regardless of perturbation levels. Moreover, larger step sizes tend to yield better performance. We also find that the step size η_P for the position variable is far more pivotal than η_Γ for the direction variable. Incidentally, the estimated best step sizes $(\eta_P^*, \eta_\Gamma^*) \approx (21.096, 17.656)$ does not coincide well with the best one found experimentally. This could be attributed to the fact that the residual reduction inequality (32) is not necessarily tight and the terms other than $q_1(\eta)$ and $q_2(\eta)$ in the contraction matrix $A(\eta)$ might not

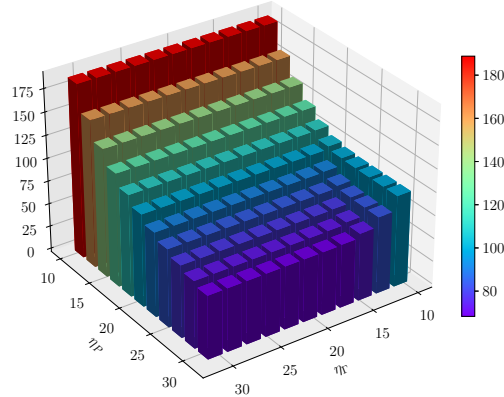
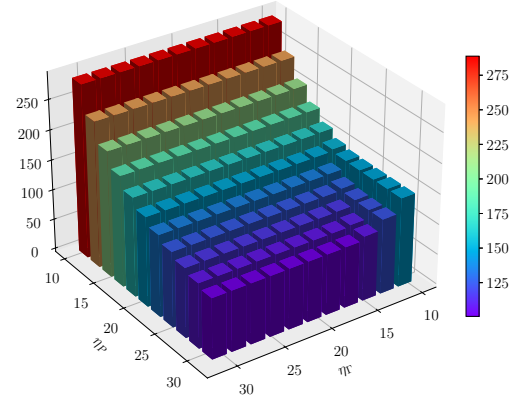
Averaged iteration number (perturb = 10^{-3})Averaged iteration number (perturb = 10^{-1})

Figure 4: Average iteration number vs (η_P, η_Γ) on the linear eigenvalue problem ($n = 10$, $p = 2$, and $\xi = 1.01$). Left: perturbation level of 10^{-3} . Right: perturbation level of 10^{-1} .

be negligible. Nevertheless, the algorithm performance with $(\eta_P^*, \eta_\Gamma^*)$ is already reasonably satisfactory.

Computation of higher-index constrained SPs. We proceed to compute the constrained SPs of all indices for an instance. We fix the problem data to be $n = 10$, $p = 2$, and $\xi = 1.01$ and the step sizes to be $\eta_P = \eta_\Gamma = 25$. The possible index of the constrained SP on this instance is at most 15. For each index in $\{0, \dots, 15\}$, we perform 200 runs of Algorithm 2 from randomly generated initial points (random seed = $0 \sim 199$). The indices and the function values at the obtained constrained SPs as well as the required iterations on average are listed in Table 2. The configurations of eigenvalues of A corresponding to the function values are also included. All the constrained SPs are found correctly and robustly (cf. Example 2). Note that the “index-0” and “index-15” constrained SPs for this example are exactly the global minimizer and maximizer, respectively.

5.2 Electronic excited-state calculations

The core of electronic calculations for molecular systems is the electronic Schrödinger equation (ESE) [75], which is in fact a linear eigenvalue problem. Nevertheless, the ESE is intractable in general due to the curse of dimensionality. For the numerical purpose, various approximations have been proposed in some atomic-orbital basis, such as the full configuration interaction (FCI), Hartree-Fock (HF) methods, and post-HF methods [40], among others. Excited states define the optical and reaction properties of atoms and molecules [5, 61, 83]. Characterizing the excited states is challenging due to electron correlation effects [32]. Finding the constrained SPs of the quantum chemical approximated methods in use arises as a natural methodology [14–16, 51, 63, 73]. Moreover, these approximations usually come together with manifold structures. In the following, we briefly introduce the HF methods and report the numerical results of finding constrained SPs as candidates of excited states, with FCI calculations (performed by PySCF [80]) as reference. More advanced levels of theory, such as the complete active space self-consistent field method [72], involve complicated manifolds and are investigated in a parallel work. Before proceeding, we remark that our methodology falls into the class of state-specific methods in quantum chemistry for electronic excited states; other popular ones include linear response theory [17, 19, 34, 67] and state-average methods for multiconfigurational approximations [85].

The HF methods. The HF approximation restricts the electronic wavefunction to a single Slater determinant parametrized by orthonormal molecular orbitals [29, 36]. In this work, we consider the restricted HF (in short, RHF) method. The RHF method assumes all molecular

Table 2: Indices, function values, the corresponding configurations of eigenvalues of A , and the needed iterations on average for finding constrained SPs on the linear eigenvalue problem ($n = 10$, $p = 2$, and $\xi = 1.01$). The configurations are indicated by doublets; e.g., (1, 3) means that the the function value equals $\frac{1}{2}(\sigma_1 + \sigma_3)$.

Indices	Func. vals.	Configs.	Iters.	Indices	Func. vals.	Configs.	Iters.
0	0.918912	(1, 2)	144.3	8	0.956223	(5, 6)	150.1
					0.956318	(4, 7)	155.5
					0.956507	(3, 8)	156.2
					0.956791	(2, 9)	162.9
					0.957170	(1, 10)	142.0
1	0.923529	(1, 3)	154.1	9	0.961028	(5, 7)	153.9
					0.961171	(4, 8)	156.2
					0.961409	(3, 9)	154.4
					0.961742	(2, 10)	150.0
2	0.928101	(2, 3)	152.5	10	0.965785	(6, 7)	148.6
					0.965881	(5, 8)	152.9
	0.928193	(1, 4)	155.8		0.966072	(4, 9)	153.0
					0.966359	(3, 10)	156.3
3	0.932764	(2, 4)	160.3	11	0.970638	(6, 8)	151.4
					0.970782	(5, 9)	152.7
	0.932903	(1, 5)	155.2		0.971023	(4, 10)	149.1
4	0.937382	(3, 4)	152.7	12	0.975443	(7, 8)	147.2
	0.937474	(2, 5)	156.2		0.975540	(6, 9)	150.4
	0.937660	(1, 6)	156.2		0.975733	(5, 10)	149.9
5	0.942092	(3, 5)	156.8	13	0.980345	(7, 9)	151.0
	0.942232	(2, 6)	155.5		0.980490	(6, 10)	149.0
	0.942465	(1, 7)	153.3				
6	0.946755	(4, 5)	151.3	14	0.985198	(8, 9)	146.2
	0.946849	(3, 6)	157.6		0.985295	(7, 10)	148.2
	0.947037	(2, 7)	154.5				
	0.947318	(1, 8)	147.1				
7	0.951513	(4, 6)	155.9	15	0.990148	(8, 10)	147.3
	0.951654	(3, 7)	157.9				
	0.951890	(2, 8)	156.1				
	0.952219	(1, 9)	163.3				

orbitals to be doubly occupied, by one spin-up and one spin-down electron. As a result, the spatial orbitals are considered to be the same for both spin-up and spin-down electrons. The spatial orbitals are expressed as the linear combinations of chosen atomic-orbitals, with the coefficients to be determined. The atomic-orbitals are assumed to be real hereafter.

For a closed-shell system with $N_{\text{elec}} \in \mathbb{N}$ electrons, the RHF approximation gives rise to the following energy functional over the Grassmann manifold:

$$E^{\text{RHF}}(\gamma) := 2\text{Tr}(h\gamma) + \text{Tr}((2J(\gamma) - K(\gamma))\gamma) \quad \text{with } \gamma \in \text{Gr}_{N_{\text{o}}}(\mathbb{R}^{N_{\text{b}}}),$$

where $N_{\text{b}} \in \mathbb{N}$ is the size of real atomic-orbital basis $\{\phi_i\}_{i=1}^{N_{\text{b}}}$, $N_{\text{o}} \in \mathbb{N}$ the number of occupied molecular orbitals ($2N_{\text{o}} = N_{\text{elec}}$), $h \in \mathbb{R}_{\text{sym}}^{N_{\text{b}} \times N_{\text{b}}}$ the discretized one-body Hamiltonian, and γ the discretized one-body reduced density matrix. Here, $J, K : \mathbb{R}_{\text{sym}}^{N_{\text{b}} \times N_{\text{b}}} \rightarrow \mathbb{R}_{\text{sym}}^{N_{\text{b}} \times N_{\text{b}}}$ are respectively the Coulomb and exchange functionals, defined as

$$[J(\gamma)]_{pq} := \sum_{r,s=1}^{N_{\text{b}}} g_{pqrs} \gamma_{sr}, \quad [K(\gamma)]_{pq} := \sum_{r,s=1}^{N_{\text{b}}} g_{psrq} \gamma_{sr}, \quad p, q = 1, \dots, N_{\text{b}},$$

with

$$g_{pqrs} := \int_{\mathbb{R}^3} \int_{\mathbb{R}^3} \frac{\phi_p(\mathbf{r})\phi_q(\mathbf{r})\phi_r(\mathbf{r}')\phi_s(\mathbf{r}')}{|\mathbf{r} - \mathbf{r}'|} d\mathbf{r} d\mathbf{r}', \quad p, q, r, s = 1, \dots, N_{\text{b}}$$

the two-body integrals.

Implementation details. We consider the H_2 and LiH molecules. The bond length of the H_2 molecule is varied from 0.1 bohr² to 4.0 bohr with a spacing of 0.1 bohr, while that of

²1 bohr $\approx 5.29 \times 10^{-11}$ m.

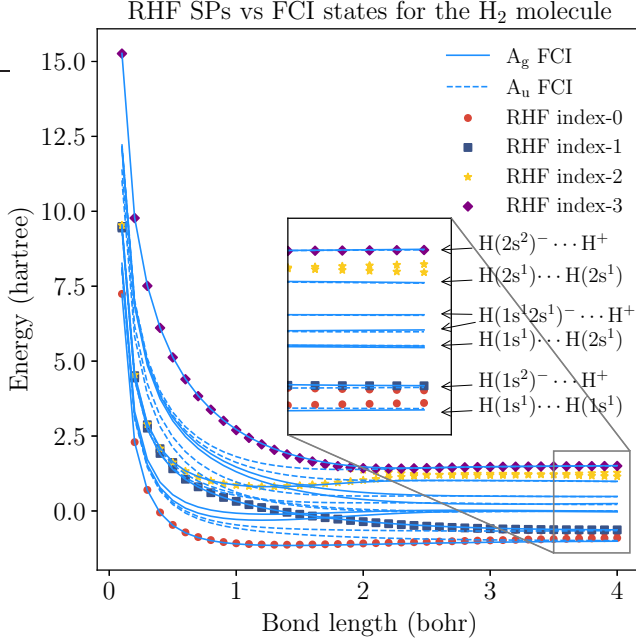


Figure 5: An overview of the constrained SPs of RHF found across the bond length interval on the H_2 molecule. The blue solid and dashed lines represent the energies of FCI states belonging to the irreps A_g and A_u , respectively. The red dots, deepblue squares, yellow stars, and purple diamonds stand for the energies of the RHF SPs of indices 0, 1, 2, and 3, respectively. The zoom-in inset describes the FCI states by atomic fragments when the molecule is close to its dissociation limit.

the LiH molecule is from 2.0 bohr to 6.0 bohr with a spacing of 0.2 bohr. The H_2 and LiH molecules are described by RHF with the 6-31G basis set ($N_{\text{elec}} = 2$, $N_b = 4$, $N_o = 1$) [24, 37] and the STO-3G basis set ($N_{\text{elec}} = 4$, $N_b = 6$, $N_o = 2$) [38], respectively. The numbers of total degrees of freedom (DOFs) are thus $N_o(N_b - N_o) = 3$ for the H_2 molecule and 8 for the LiH molecule. We investigate the energy landscape of RHF for both molecules with the varying bond lengths by searching for the constrained SPs of allowed indices. They are found by running Algorithm 2 from 1,000 random initial points (random seed = 0 \sim 999); see the pseudocodes in Section 5.1 for initialization. For retraction, Algorithm 2 is equipped with the exponential mapping for the position part; the treatment for the direction part is similar to that in the previous subsection. The step size is specified as $\eta = 10^{-1}$ and $\eta = 10^{-2}$ for the H_2 and LiH molecules, respectively, which are not necessarily optimal. The maximum iteration number and convergence tolerance are respectively set as $\text{maxit} = \infty$ and $\text{tol} = 10^{-6}$. The results are compared with those obtained by solving FCI based on the RHF ground-state calculations, which is exact under the basis in use. In particular, FCI gives 16 states for the H_2 molecule and 225 states for the LiH molecule.

Results on the H_2 molecule. An overview of the constrained SPs of RHF identified across the considered bond length interval is shown in Figure 5, together with the ground-/excited-state energies of FCI as reference. It can be seen that the RHF energy landscape varies smoothly with the bond length. Note that FCI states are classified by their irreducible representations (irreps); for the H_2 molecule in the computational point group D_{2h} , the relevant irreps are A_g and A_u , with eight FCI states belonging to each. It is observed that the RHF SPs are only able to describe a small subset (e.g., four near the equilibrium geometry, three close to the dissociation limit) of FCI states in terms of their energies. This behavior is consistent with the fact that RHF neglects electronic correlation [8]. The deficiency can be mitigated to

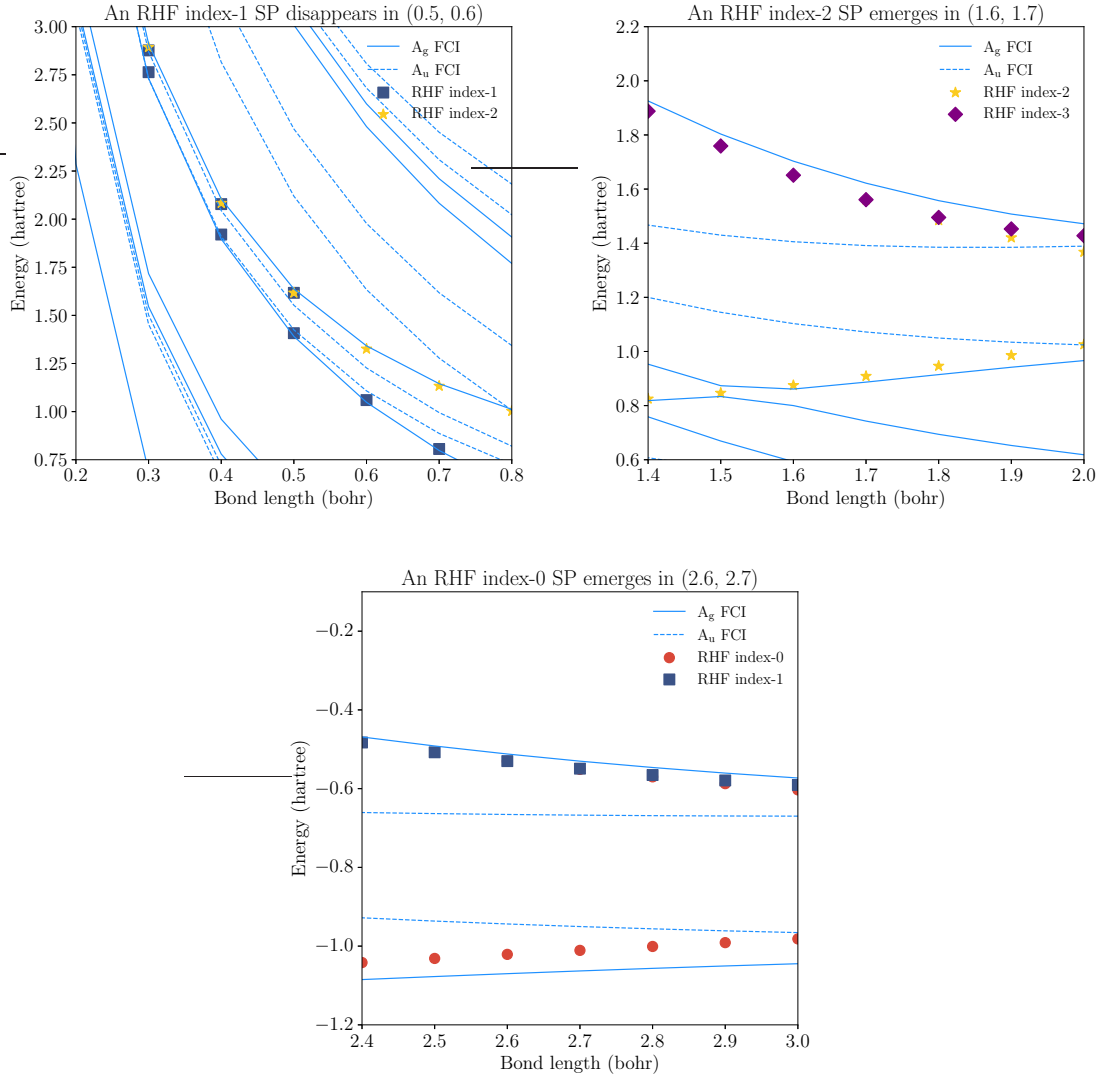


Figure 6: Zoom-in views of the constrained SPs of RHF. Upper left: an RHF index-1 SP disappears in (0.5 bohr, 0.6 bohr). Upper right: an RHF index-2 SP emerges in (1.6 bohr, 1.7 bohr). Lower: an RHF index-0 SP emerges in (2.6 bohr, 2.7 bohr).

some extent by resorting to post-HF methods, which is investigated in a parallel work.

Our results also reveal numerically that the varying bond length, as an external parameter, can lead to disappearance or emergence of constrained SPs. Zoom-in views are given in Figure 6. Concretely, in the interval (0.5 bohr, 0.6 bohr), an index-1 SP gets close to the index-2 SP, in terms of energy, and disappears; in the interval (1.6 bohr, 1.7 bohr), an index-2 SP close to the index-3 SP emerges; and in the interval (2.6 bohr, 2.7 bohr), an index-0 SP (i.e., a local minimizer) close to the index-1 SP emerges.

Results on the LiH molecule. The identified constrained SPs of RHF are shown in a similar way in Figure 7, again with the FCI states energies as reference. For the LiH molecule in the computational group C_{2v} , the relevant irreps are A_1 , A_2 , B_1 , and B_2 . Note that the B_1 and B_2 FCI states are two-fold degenerate across the considered bond length interval. In this case, the RHF SPs appear to well describe the low-lying FCI states with energies lower than -6 hartree³. But the FCI states with energies in $(-6$ hartree, -4 hartree) are completely missed by the RHF SPs, probably due to inherent shortcomings of the RHF

³1 hartree $\approx 4.36 \times 10^{-18}$ J

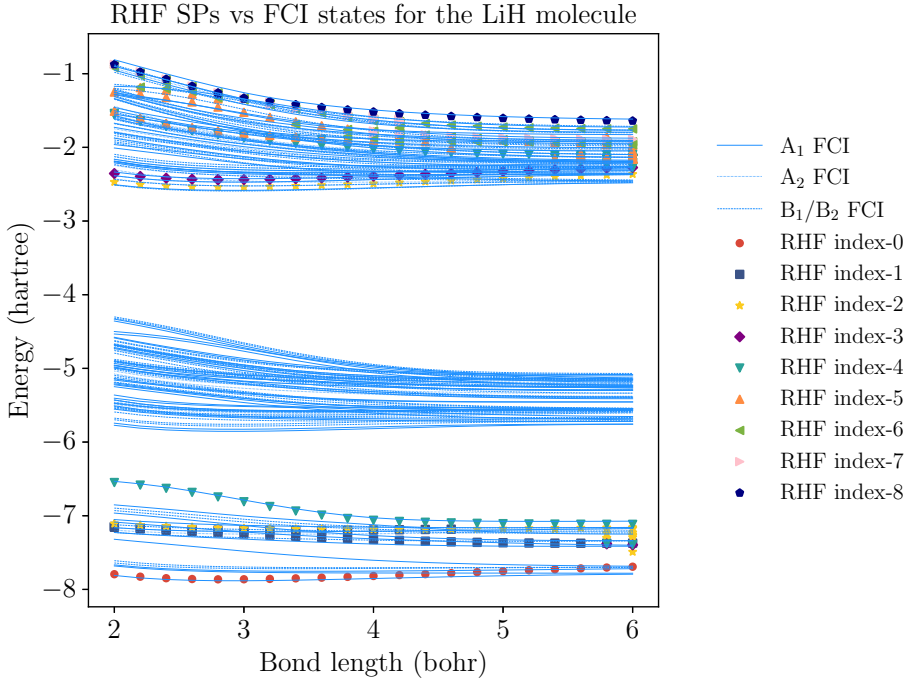


Figure 7: An overview of the constrained SPs of RHF found across the bond length interval on the LiH molecule. The blue solid, dotted, and dashed lines represent the energies of FCI states belonging to the irreps A_1 , A_2 , B_1 (or B_2), respectively. The red dots, deepblue squares, yellow stars, purple diamonds, down-pointing cyan triangles, up-pointing orange triangles, left-pointing green triangles, right-pointing pink triangles, and navyblue pentagons stand for the energies of the RHF SPs of indices 0 to 8, respectively.

approximation. In addition, the potential energy surfaces of higher-index RHF SPs are found to be more complicated than those of low-index SPs, especially when the molecule is driven to the dissociation limit.

The above results provide proof-of-concept evidence for the effectiveness of our algorithms in excited-state calculations. Nonetheless, we shall point out that a comprehensive quantum chemical analysis of the obtained SPs, though beyond the scope of present work, is essential for practical applications. As a nonlinear approximation to the exact theory, RHF may produce critical points that lack physical meanings; e.g., a spurious non-global local minimizer emerges when the bond length exceeds 2.7 bohr in the right panel of Figure 6. Moreover, since RHF is a low-dimensional approximation, a one-to-one correspondence between RHF SPs and excited states in the same energetic order no longer holds. Molecular geometries must also be taken into account. In the exact theory, the ESE is parameterized by atomic configurations. Variations in molecular geometry may induce degeneracies and crossings in states, which would lead to unfavorable features of potential energy surfaces within approximate theories (cf. Figure 6). From the computational aspect, it is of great importance to develop schemes capable of efficiently navigating the nonconvex landscape [86], instead of relying on random multi-start.

6 Conclusions

We have developed a constrained saddle dynamics for finding SPs on general Riemannian manifolds. The dynamics is formulated compactly over the Grassmann bundle of the tangent bundle, and achieves broad applicability by incorporating the second fundamental form, which

captures variations of tangent spaces along the trajectory. By investigating the Grassmann bundle geometry, we have rigorously established the theoretical properties of both the dynamics and the resulting discretized algorithms. Remarkably, our analysis provides the first linear convergence results of the discretized algorithms in manifold settings. Moreover, compared with existing results, we eliminate unnecessary nondegeneracy assumptions on the eigenvalues of the Riemannian Hessian by adopting a single orthogonal projector as the direction variable, thereby respecting the underlying quotient structure. We have also characterized how the spectrum of the Riemannian Hessian affects the local convergence rates and highlighted the importance of using nonredundant parametrizations. Both of these two points have been validated through numerical results on linear eigenvalues problems. Finally, we have applied the proposed algorithms to electronic excited-state calculations.

There remains lots of directions to be explored. The numerical performance of the discretized algorithms is highly sensitive to condition numbers, as evidenced by their local convergence rates. It is thus desirable to incorporate higher-order contributions without sacrificing local convergence properties. In addition, a globally convergent method for locating SPs on Riemannian manifolds is still lacking, due to the absence of a global merit function. One possible avenue is to extend the analysis in [49] and develop stochastic methods on manifolds. From the perspective of quantum chemistry, it would also be valuable to investigate the manifold geometry underlying more complicated levels of theory and to devise efficient yet physically meaningful strategies for navigating the associated nonconvex energy landscapes.

Acknowledgements

This work has received funding from the European Research Council (ERC) under the European Union’s Horizon 2020 research and innovation program (grant agreement EMC2 No 810367). The authors are grateful to Éric Cancès, Tony Lelièvre, and Panos Parpas for useful discussions.

References

- [1] P.-A. Absil, R. Mahony, and R. Sepulchre, *Optimization Algorithms on Matrix Manifolds*, Princeton University Press, 2008.
- [2] A. Ambrosetti and P. H. Rabinowitz, *Dual variational methods in critical point theory and applications*, J. Funct. Anal. **14** (1973), no. 4, 349–381.
- [3] D. Arrowsmith and C. M. Place, *Dynamical Systems: Differential Equations, Maps, and Chaotic Behaviour*, Chapman & Hall, 1992.
- [4] J. Baker, *An algorithm for the location of transition states*, J. Comput. Chem. **7** (1986), no. 4, 385–395.
- [5] V. Balzani, P. Ceroni, and A. Juris, *Photochemistry and Photophysics: Concepts, Research, Applications*, John Wiley & Sons, 2014.
- [6] A. Banerjee, N. Adams, J. Simons, and R. Shepard, *Search for stationary points on surfaces*, J. Phys. Chem. **89** (1985), no. 1, 52–57.
- [7] W. Bao and Y. Cai, *Mathematical theory and numerical methods for Bose-Einstein condensation*, Kinet. Relat. Models **6** (2013), no. 1, 1–135.
- [8] G. M. J. Barca, A. T. B. Gilbert, and P. M. W. Gill, *Communication: Hartree-Fock description of excited states of H_2* , J. Chem. Phys. **141** (2014), no. 11, 111104.
- [9] G. T. Barkema and N. Mousseau, *Event-based relaxation of continuous disordered systems*, Phys. Rev. Lett. **77** (1996), no. 21, 4358.
- [10] ———, *The activation–relaxation technique: an efficient algorithm for sampling energy landscapes*, Comput. Mater. Sci. **20** (2001), no. 3-4, 285–292.
- [11] T. Bendokat, R. Zimmermann, and P.-A. Absil, *A Grassmann manifold handbook: basic geometry and computational aspects*, Adv. Comput. Math. **50** (2024), no. 1, 6.
- [12] S. N. Bose, *Plancks gesetz und lichtquantenhypothese*, Z. Angew. Phys. **26** (1924), no. 1, 178–181.
- [13] N. Boumal, *An Introduction to Optimization on Smooth Manifolds*, Cambridge University Press, 2023.

- [14] H. G. A. Burton, *Energy landscape of state-specific electronic structure theory*, J. Chem. Theory Comput. **18** (2022), no. 3, 1512–1526.
- [15] H. G. A. Burton and D. J. Wales, *Energy landscapes for electronic structure*, J. Chem. Theory Comput. **17** (2020), no. 1, 151–169.
- [16] E. Cancès, H. Galicher, and M. Lewin, *Computing electronic structures: a new multiconfiguration approach for excited states*, J. Comput. Phys. **212** (2006), no. 1, 73–98.
- [17] E. Cancès and C. Le Bris, *On the time-dependent Hartree-Fock equations coupled with a classical nuclear dynamics*, Math. Models Methods Appl. Sci. **9** (1999), no. 07, 963–990.
- [18] E. Cancès, F. Legoll, M.-C. Marinica, K. Minoukadeh, and F. Willaime, *Some improvements of the activation-relaxation technique method for finding transition pathways on potential energy surfaces*, J. Chem. Phys. **130** (2009), no. 11, 114711.
- [19] M. E. Casida, *Time-dependent density functional response theory for molecules*, Recent advances in density functional methods: (part i), 1995, pp. 155–192.
- [20] C. J. Cerjan and W. H. Miller, *On finding transition states*, J. Chem. Phys. **75** (1981), no. 6, 2800–2806.
- [21] M. T. Chu and M. M. Lin, *Generalized gentlest ascent dynamics methods for high-index saddle points*, SIAM J. Numer. Anal. **63** (2025), no. 6, 2343–2370.
- [22] G. M. Crippen and H. A. Scheraga, *Minimization of polypeptide energy: XI. The method of gentlest ascent*, Arch. Biochem. Biophys. **144** (1971), no. 2, 462–466.
- [23] G. Cui, K. Jiang, and T. Zhou, *An efficient saddle search method for ordered phase transitions involving translational invariance*, Comput. Phys. Commun. **306** (2025), 109381.
- [24] R. H. W. J. Ditchfield, W. J. Hehre, and J. A. Pople, *Self-consistent molecular-orbital methods. IX. An extended Gaussian-type basis for molecular-orbital studies of organic molecules*, J. Chem. Phys. **54** (1971), no. 2, 724–728.
- [25] J. P. K. Doye and D. J. Wales, *Surveying a potential energy surface by eigenvector-following: applications to global optimisation and the structural transformations of clusters*, Z. Phys. D: At. Mol. Clusters **40** (1997), 194–197.
- [26] W. E and X. Zhou, *The gentlest ascent dynamics*, Nonlinearity **24** (2011), no. 6, 1831.
- [27] A. Edelman, T. A. Arias, and S. T. Smith, *The geometry of algorithms with orthogonality constraints*, SIAM J. Matrix Anal. Appl. **20** (1998), no. 2, 303–353.
- [28] A. Einstein, *Quantentheorie des einatomigen idealen gases. Zweite abhandlung*, Sitzungsber. K. Preuss. Akad. Wiss. **1** (1925), 3–14.
- [29] V. Fock, *Näherungsmethode zur lösung des quantenmechanischen mehrkörperproblems*, Z. Angew. Phys. **61** (1930), no. 1, 126–148.
- [30] W. Gao, J. Leng, and X. Zhou, *An iterative minimization formulation for saddle point search*, SIAM J. Numer. Anal. **53** (2015), no. 4, 1786–1805.
- [31] M. Goldstein, *Viscous liquids and the glass transition: a potential energy barrier picture*, J. Chem. Phys. **51** (1969), no. 9, 3728–3739.
- [32] L. González, D. Escudero, and L. Serrano-Andrés, *Progress and challenges in the calculation of electronic excited states*, ChemPhysChem **13** (2012), no. 1, 28–51.
- [33] N. I. M. Gould, C. Ortner, and D. Packwood, *A dimer-type saddle search algorithm with preconditioning and linesearch*, Math. Comput. **85** (2016), no. 302, 2939–2966.
- [34] L. Grazioli, Y. Hu, and E. Cancès, *Critical point search and linear response theory for computing electronic excitation energies of molecular systems. Part I: general framework, application to Hartree-Fock and DFT*, J. Chem. Phys. (2026+), in press.
- [35] S. Gu, X. Zhang H. Zhang, and X. Zhou, *Iterative Proximal-Minimization for Computing Saddle Points with Fixed Index*, 2025.
- [36] D. R. Hartree, *The wave mechanics of an atom with a non-Coulomb central field. Part I. Theory and methods*, Math. Proc. Cambridge Philos. Soc. **24** (1928), no. 1, 89–110.
- [37] W. J. Hehre, R. H. W. J. Ditchfield, and J. A. Pople, *Self-consistent molecular orbital methods. XII. Further extensions of Gaussian-type basis sets for use in molecular orbital studies of organic molecules*, J. Chem. Phys. **56** (1972), no. 5, 2257–2261.
- [38] W. J. Hehre, R. F. Stewart, and J. A. Pople, *Self-consistent molecular-orbital methods. I. Use of Gaussian expansions of Slater-type atomic orbitals*, J. Chem. Phys. **51** (1969), no. 6, 2657–2664.
- [39] D. Heidrich and W. Quapp, *Saddle points of index 2 on potential energy surfaces and their role in theoretical reactivity investigations*, Theor. Chim. Acta **70** (1986), no. 2, 89–98.

[40] T. Helgaker, P. Jørgensen, and J. Olsen, *Molecular Electronic-Structure Theory*, 1st ed., John Wiley & Sons, Ltd, 2000.

[41] G. Henkelman, G. Jóhannesson, and H. Jónsson, *Methods for finding saddle points and minimum energy paths*, Theoretical methods in condensed phase chemistry, 2002, pp. 269–302.

[42] G. Henkelman and H. Jónsson, *A dimer method for finding saddle points on high dimensional potential surfaces using only first derivatives*, J. Chem. Phys. **111** (1999), no. 15, 7010–7022.

[43] K. Jiang, L. Zhang, X. Zheng, and T. Zhou, *Nullspace-Preserving High-Index Saddle Dynamics Method for Degenerate Multiple Solution Problems*, 2025.

[44] J. Kästner and P. Sherwood, *Superlinearly converging dimer method for transition state search*, J. Chem. Phys. **128** (2008), no. 1, 014106.

[45] E. F. Koslover and D. J. Wales, *Comparison of double-ended transition state search methods*, J. Chem. Phys. **127** (2007), no. 13, 134102.

[46] C. Lanczos, *An iteration method for the solution of the eigenvalue problem of linear differential and integral operators*, J. Res. Natl. Bur. Stand. **45** (1950), no. 4, 255–282.

[47] J. M. Lee, *Introduction to Smooth Manifolds*, 2nd ed., Graduate Texts in Mathematics, vol. 218, Springer New York, NY, 2012 (en).

[48] ———, *Introduction to Riemannian Manifolds*, 2nd ed., Graduate Texts in Mathematics, vol. 176, Springer Cham, 2018.

[49] T. Lelièvre and P. Parpas, *Using Witten Laplacians to locate index-1 saddle points*, SIAM J. Sci. Comput. **46** (2024), no. 2, A770–A797.

[50] A. Levitt and C. Ortner, *Convergence and cycling in walker-type saddle search algorithms*, SIAM J. Numer. Anal. **55** (2017), no. 5, 2204–2227.

[51] M. Lewin, *Solutions of the multiconfiguration equations in quantum chemistry*, Arch. Ration. Mech. Anal. **171** (2004), no. 1, 83–114.

[52] C. Li, J. Lu, and W. Yang, *Gentlest ascent dynamics for calculating first excited state and exploring energy landscape of Kohn-Sham density functionals*, J. Chem. Phys. **143** (2015), no. 22, 224110.

[53] Y. Li and J. Zhou, *A minimax method for finding multiple critical points and its applications to semilinear PDEs*, SIAM J. Sci. Comput. **23** (2001), no. 3, 840–865.

[54] W. Liu, Z. Xie, and Y. Yuan, *A constrained gentlest ascent dynamics and its applications to finding excited states of Bose-Einstein condensates*, J. Comput. Phys. **473** (2023), 111719.

[55] X. Liu, H. Chen, and C. Ortner, *Stability of the minimum energy path*, Numer. Math. **156** (2024), no. 1, 39–70.

[56] Y. Liu, H. Su, Z. Xiao, L. Zhang, and J. Zhao, *SaddleScape V1.0: a Python Package for Constructing Solution Landscapes via High-Index Saddle Dynamics*, 2026.

[57] Y. Luo, L. Zhang, P. Zhang, Z. Zhang, and X. Zheng, *Semi-implicit method of high-index saddle dynamics and application to construct solution landscape*, Numer. Methods Partial Differ. Equations **40** (2024), no. 6, e23123.

[58] Y. Luo, L. Zhang, and X. Zheng, *Accelerated high-index saddle dynamics method for searching high-index saddle points*, J. Sci. Comput. **102** (2025), no. 2, 31.

[59] Y. Luo, X. Zheng, X. Cheng, and L. Zhang, *Convergence analysis of discrete high-index saddle dynamics*, SIAM J. Numer. Anal. **60** (2022), no. 5, 2731–2750.

[60] E. Machado-Charry, L. K. Béland, D. Caliste, L. Genovese, T. Deutsch, N. Mousseau, and P. Pochet, *Optimized energy landscape exploration using the ab initio based activation-relaxation technique*, J. Chem. Phys. **135** (2011), no. 3, 034102.

[61] S. Mai and L. González, *Molecular photochemistry: recent developments in theory*, Angew. Chem. Int. Ed. **59** (2020), no. 39, 16832–16846.

[62] R. Malek and N. Mousseau, *Dynamics of Lennard-Jones clusters: a characterization of the activation-relaxation technique*, Phys. Rev. E **62** (2000), no. 6, 7723.

[63] A. Marie and H. G. A. Burton, *Excited states, symmetry breaking, and unphysical solutions in state-specific CASSCF theory*, J. Phys. Chem. A **127** (2023), no. 20, 4538–4552.

[64] D. Mehta, J. Chen, D. Z. Chen, H. Kusumaatmaja, and D. J. Wales, *Kinetic transition networks for the Thomson problem and Smale’s seventh problem*, Phys. Rev. Lett. **117** (2016), no. 2, 028301.

[65] R. A. Miron and K. A. Fitchhorn, *The step and slide method for finding saddle points on multidimensional potential surfaces*, J. Chem. Phys. **115** (2001), no. 19, 8742–8747.

[66] E. Musso and F. Tricerri, *Riemannian metrics on tangent bundles*, Ann. Mat. Pura Appl. **150** (1988), no. 1, 1–19.

[67] J. Olsen and P. Jørgensen, *Linear and nonlinear response functions for an exact state and for an MCSCF state*, J. Chem. Phys. **82** (1985), no. 7, 3235–3264.

[68] R. A. Olsen, G. J. Kroes, G. Henkelman, A. Arnaldsson, and H. Jónsson, *Comparison of methods for finding saddle points without knowledge of the final states*, J. Chem. Phys. **121** (2004), no. 20, 9776–9792.

[69] M. C. Payne, M. P. Teter, D. C. Allan, T. A. Arias, and J. D. Joannopoulos, *Iterative minimization techniques for ab initio total-energy calculations: molecular dynamics and conjugate gradients*, Rev. Mod. Phys. **64** (1992), no. 4, 1045.

[70] A. Poddey and P. E. Blöchl, *Dynamical dimer method for the determination of transition states with ab initio molecular dynamics*, J. Chem. Phys. **128** (2008), no. 4, 044107.

[71] W. Quapp and J. M. Bofill, *Locating saddle points of any index on potential energy surfaces by the generalized gentlest ascent dynamics*, Theor. Chem. Acc. **133** (2014), 1–14.

[72] B. O. Roos, P. R. Taylor, and P. E. M. Sigbahn, *A complete active space SCF method (CASSCF) using a density matrix formulated super-CI approach*, Chem. Phys. **48** (1980), no. 2, 157–173.

[73] S. Saade and H. G. A. Burton, *Excited state-specific CASSCF theory for the torsion of ethylene*, J. Chem. Theory Comput. **20** (2024), no. 12, 5105–5114.

[74] S. Sasaki, *On the differential geometry of tangent bundles of Riemannian manifolds*, Tohoku Math. J. (Second Ser.) **10** (1958), no. 3, 338–354.

[75] E. Schrödinger, *An undulatory theory of the mechanics of atoms and molecules*, Phys. Rev. **28** (1926), no. 6, 1049.

[76] E. Shakhnovich, V. Abkevich, and O. Ptitsyn, *Conserved residues and the mechanism of protein folding*, Nature **379** (1996), no. 6560, 96–98.

[77] B. Shi, L. Zhang, and Q. Du, *A Stochastic Algorithm for Searching Saddle Points with Convergence Guarantee*, 2025.

[78] J. Simons, P. Jørgensen, H. Taylor, and J. Ozment, *Walking on potential energy surfaces*, J. Phys. Chem. **87** (1983), 2745–2753 (en).

[79] H. Su, H. Wang, L. Zhang, J. Zhao, and X. Zheng, *Improved high-index saddle dynamics for finding saddle points and solution landscape*, SIAM J. Numer. Anal. **63** (2025), no. 4, 1757–1775.

[80] Q. Sun, X. Zhang, S. Banerjee, P. Bao, M. Barbry, N. S. Blunt, N. A. Bogdanov, G. H. Booth, J. Chen, Z.-H. Cui, J. J. Eriksen, Y. Gao, S. Guo, J. Hermann, M. R. Hermes, K. Koh, P. Koval, S. Lehtola, Z. Li, J. Liu, N. Mardirossian, J. D. McClain, M. Motta, B. Mussard, H. Q. Pham, A. Pulkin, W. Purwanto, P. J. Robinson, E. Ronca, E. R. Sayfutyarova, M. Scheurer, H. F. Schurkus, J. E. T. Smith, C. Sun, S.-N. Sun, S. Upadhyay, L. K. Wagner, X. Wang, A. White, J. D. Whitfield, M. J. Williamson, S. Wouters, J. Yang, J. M. Yu, T. Zhu, T. C. Berkelbach, S. Sharma, A. Y. Sokolov, and G. K.-L. Chan, *Recent developments in the PySCF program package*, J. Chem. Phys. **153** (2020), no. 2, 024109.

[81] J. J. Thomson, *On the structure of the atom: an investigation of the stability and periods of oscillation of a number of corpuscles arranged at equal intervals around the circumference of a circle; with application of the results to the theory of atomic structure*, Lond. Edinb. Dubl. Phil. Mag. **7** (1904), no. 39, 237–265.

[82] D. G. Truhlar, B. C. Garrett, and S. J. Klippenstein, *Current status of transition-state theory*, J. Phys. Chem. **100** (1996), no. 31, 12771–12800.

[83] N. J. Turro, V. Ramamurthy, and J. C. Scaiano, *Principles of Molecular Photochemistry: an Introduction*, University Science Books, 2009.

[84] L. Vidal, T. Nottoli, F. Lipparini, and E. Cancès, *Geometric optimization of restricted-open and complete active space self-consistent field wave functions*, J. Phys. Chem. A **128** (2024), no. 31, 6601–6612.

[85] H.-J. Werner and W. Meyer, *A quadratically convergent MCSCF method for the simultaneous optimization of several states*, J. Chem. Phys. **74** (1981), no. 10, 5794–5801.

[86] Q. Xu and A. Delin, *A General Optimization Framework for Mapping Local Transition-State Networks*, 2025.

[87] J. Yin, Z. Huang, and L. Zhang, *Constrained high-index saddle dynamics for the solution landscape with equality constraints*, J. Sci. Comput. **91** (2022), no. 2, 62.

[88] J. Yin, B. Yu, and L. Zhang, *Searching the solution landscape by generalized high-index saddle dynamics*, Sci. China Math. **64** (2021), no. 8, 1801–1816.

[89] J. Yin, L. Zhang, and P. Zhang, *High-index optimization-based shrinking dimer method for finding high-index saddle points*, SIAM J. Sci. Comput. **41** (2019), no. 6, A3576–A3595.

[90] J. Zhang and Q. Du, *Constrained shrinking dimer dynamics for saddle point search with constraints*, J. Comput. Phys. **231** (2012), no. 14, 4745–4758.

[91] ———, *Shrinking dimer dynamics and its applications to saddle point search*, SIAM J. Numer. Anal. **50** (2012), no. 4, 1899–1921.

- [92] L. Zhang, Q. Du, and Z. Zheng, *Optimization-based shrinking dimer method for finding transition states*, SIAM J. Sci. Comput. **38** (2016), no. 1, A528–A544.
- [93] L. Zhang, P. Zhang, and X. Zheng, *Error estimates for Euler discretization of high-index saddle dynamics*, SIAM J. Numer. Anal. **60** (2022), no. 5, 2925–2944.
- [94] ———, *Discretization and index-robust error analysis for constrained high-index saddle dynamics on the high-dimensional sphere*, Sci. China Math. **66** (2023), no. 10, 2347–2360.